

Supporting Information

Copper Complexes as Catalyst Precursor in the Electrochemical Hydrogen Evolution Reaction

Merle Kügler,^[a] Julius Scholz,^[b] Andreas Kronz,^[c] Inke Siewert^{[a]*}

[a] Georg-August-University Göttingen, Institute of Inorganic Chemistry, Tammannstrasse 4, D-37077 Göttingen, Germany

[b] Georg-August-University Göttingen, Institut für Materialphysik, Friedrich-Hund-Platz 1, D-37077 Göttingen.

[c] Georg-August-University Göttingen, Geowissenschaftliches Zentrum, Goldschmidtstrasse 1, D-37077 Göttingen, Germany

Table of Content

1) Experimental	2
a) Instrumental details	2
b) Potentiometric Titrations	2
c) Spectrophotometric Titrations	2
A Varian Cary 50 Bio UV/Visible spectrophotometer was used in the experiments.	2
d) CPE-MS experiments	2
e) Experimental Procedures	3
2) Molecular Structure	6
a) X-ray Crystallography	6
b) Hydrogen Bond Network.....	7
3) pK _a -Determinations of the Ligands	8
a) Potentiometric Determinations of the pK _a of L ² and L ³	8
b) Spectrophotometric Titrations for the Determination of the pK _a of L ⁴	9
4) Spectrophotometric Titrations	10
a) Species Distributions of the L ¹⁻⁴ -Cu(II) Systems in MeOH/Water	10
i) Complex 3bH ₁	10
ii) Complex 4bH ₁	12
iii) Complex 1bH ₃	14
iv) Complex 2bH ₃	16
b) Species Distributions in Water	17
i) Employing L ¹	17

ii) Employing L ⁵	19
5) Electrochemical Studies	21
6) Electron Microprobe Analysis (EMPA)	27
a) Sample preparation	27
b) Measurement	27
7) XPS Measurements	29
a) Sample Preparation	29
b) Measurement	29
8) References	31

1) Experimental

a) Instrumental details

Microanalyses were performed on an *Elementar Vario El II* elemental analyser. IR spectra were recorded using samples prepared as KBr pellets with a *Bruker VERTEX 70* FTIR-spectrometer. Mass spectra were recorded on a *Bruker APEX IV micrOTOF*, or a *Bruker Autoflex Speed* mass spectrometer. UV/Vis spectra were recorded with a *Varian Cary50 Scan*. The ligands L¹ and L³ were synthesised according to previous reported literature procedures.^[1]

b) Potentiometric Titrations

The ligands L^{1[1]}, L² and L³ were studied in a mixture of MeOH/water (80/20 by weight). The ionic strength was fixed at $I = 0.1$ M with KCl. The titrations were performed using a *Metrohm 809 Titrand* system equipped in combined glass electrode (*Metrohm 6.0234.100*) filled with 0.1 M KCl (L²)/ NaCl (L³) in MeOH/water (80/20 by weight). ~0.1 M KOH solution was prepared in a MeOH/water mixture (80/20 by weight), standardised by titration with potassium hydrogen phthalate and added by a *Metrohm 800 Dosino* auto burette. The ionic product of water under the used conditions was $10^{-14.42}$ mol²dm^{3[2]}. The purity and exact concentration of the ligand were determined by the method of Gran. All titrations were carried out as 3.0 mL samples in a thermostatted cell at 25±0.2 °C under a stream of inert gas.

c) Spectrophotometric Titrations

In MeOH/water: UV/Vis spectra were collected with 1 cm optical length cuvettes. The pH values were measured by a combined glass electrode (*Metrohm 6.0234.100*) filled with 0.1 M NaCl solution (MeOH/water, 80/20 by weight). The spectra were collected in 2.5 mL samples.

In water: UV/Vis spectra were collected with 1 cm optical length cuvettes. The pH values were measured by a combined glass electrode (*Metrohm 6.0234.100*) filled with 3 M aqueous KCl solution. The spectra were collected in 2.5 mL samples.

A Varian Cary 50 Bio UV/Visible spectrophotometer was used in the experiments.

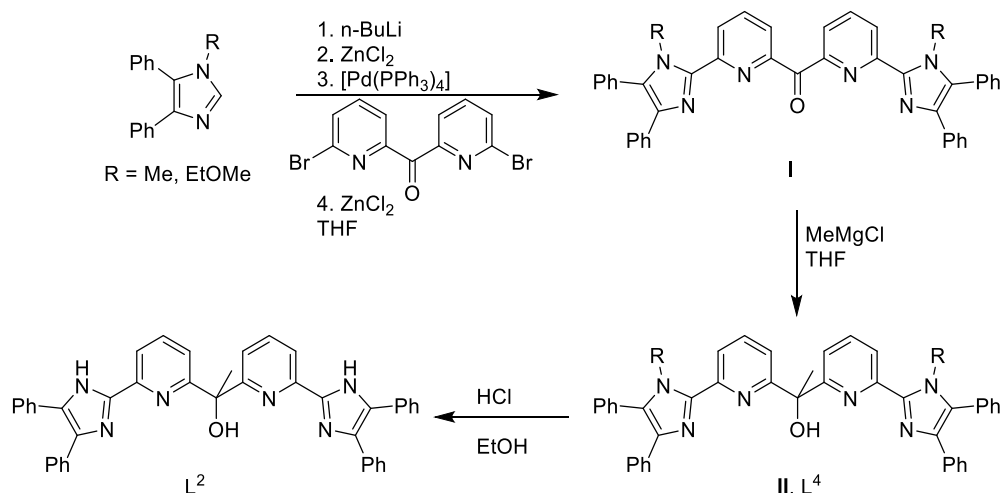
d) CPE-MS experiments

The MS was a Pfeiffer vacuum ThermoStar GSD 320 T. The MS was connect to the electrolysis cell via a thin glass capillary of ~1.5 m (heated by a heating mantel to 200°C, inlet temperature 100°C), a three-way ball valve with connections to the glass capillary, a needle and inert gas. The special set up led to

delay in the measurement. Measurements in MeCN were conducted in dry and distilled MeCN with a three electrode setup, a glassy carbon electrode as working electrode, a platinum wire as counter electrode and a silver wire as pseudo reference. The measurements were referenced by adding ferrocene to the solution.

e) Experimental Procedures

Overview on the of synthesis of the ligands L² and L⁴



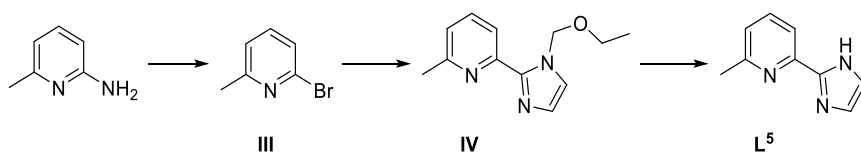
I: *n*-BuLi (1.6 M, 11 mL, 18 mmol) was added to a solution of phenylimidazole (18 mmol) dissolved in THF (50 mL) at -78 °C. After 1 h, a solution of dry ZnCl₂ (2.4 g, 18 mmol) in THF (50 mL) was added and the reaction mixture was allowed to warm to rt. Subsequently, a mixture of bis(6-bromopyridine-2-yl)methanone (2.0 g, 5.8 mmol) and Pd(PPh₃)₄ (0.34 g, 0.30 mmol) in THF (50 mL) was added and the reaction mixture stirred for 1.5 h at 60 °C in a closed vessel. The reaction mixture was cooled to rt and a solution of dry ZnCl₂ (4.8 g, 36 mmol) in THF (100 mL) was added. The reaction mixture was stirred for additional 5 h at 60 °C, then cooled down to rt and added to a solution of Na₂EDTA·2H₂O in water (0.24 M, 450 mL). The pH of the aq. phase was adjusted to 8 with aq. Na₂CO₃-solution (10%) and the crude product was extracted with dichloromethane. The combined organic phases were washed with brine and dried over MgSO₄. The solvent was removed under reduced pressure. The compounds were purified by column chromatography (silica gel, hexane/ethyl acetate 4:1 + 2 % NEt₃). a) *Bis(6-(1-(ethoxymethyl)-4,5-diphenylimidazole-2-yl)pyridine-2-yl)-methanone*, yellow powder, yield 81 % (3.4 g, 4.8 mmol). ¹H-NMR (CDCl₃): δ = 8.59 (dd, *J* = 7.1, 2.1 Hz, 2 H, H^{5-py}), 8.20-7.84 (m, 4, H^{3,4-py}), 7.55-7.44 (m, 4 H, H^{ph}), 7.42-7.34 (m, 10 H, H^{ph}), 7.25-7.13 (m, 6 H, H^{ph}), 5.61 (s, 4 H, N-CH₂-O), 3.06 (q, *J* = 7.0 Hz, 4 H, O-CH₂-Me), 0.83 (t, *J* = 7.0 Hz, 6 H, Me). ¹³C-NMR (CDCl₃): δ = 192.6 (C=O), 153.2 (C^{2/6-py}), 150.0 (C^{2/6-py}), 143.6 (C^{2-im}), 138.7 (C^{4-im}), 137.6 (C^{4-py}), 134.0 (C^{ph}), 132.6 (C^{5-im}), 131.1 (C^{ph}), 130.0 (C^{ph}), 128.8 (C^{ph}), 128.7 (C^{ph}), 128.1 (C^{ph}), 127.0 (C^{ph}), 126.6 (C^{ph}), 126.1 (C^{5-py}), 123.6 (C^{3-py}), 73.4 (N-CH₂-O), 63.4 (O-CH₂-Me), 14.7 (Me). MS (ESI+, MeCN): *m/z* = 737.3 ([M+H]⁺), 775.3 ([M+K]⁺). IR (KBr): ν (cm⁻¹) = 3057 (w), 2973 (w), 2927 (w), 1685 (s), 1602 (s), 1584 (m), 1501 (m), 1474 (s), 1442 (s), 1411 (m), 1377 (m), 1325 (m), 1267 (m), 1243 (w), 1205 (w), 1156 (w), 1097 (s), 1023 (w), 992 (w), 957 (m), 916 (w), 837 (w), 800 (w), 775 (s), 722 (m), 697 (s), 635 (w). b) *Bis(6-(1-(methyl)-4,5-diphenylimidazole-2-yl)pyridine-2-yl)-methanone*, white powder, 65 % (2.5 g, 3.8 mmol). ¹H-NMR (CDCl₃): δ = 8.56 (dd, *J* = 5.4, 3.7 Hz, 2 H, H^{5-py}), 8.00-7.98 (m, 4 H, H^{3,4-py}), 7.54-7.47 (m, 6 H, H^{ph}), 7.43-7.30 (m, 6 H, H^{ph}), 7.27-7.07 (m, 8 H, H^{ph}), 3.59 (s, 6 H, NMe). ¹³C-NMR (CDCl₃): δ = 193.1 (C=O), 153.4 (C^{2/6-py}), 150.1 (C^{2/6-py}), 143.8 (C^{2-im}), 138.3 (C^{4-im}), 137.4 (C^{3-py}), 134.4 (C^{ph}), 132.8 (C^{5-im}), 131.1 (C^{ph}), 130.9 (C^{ph}), 130.5 (C^{ph}), 129.1 (C^{ph}), 128.9 (C^{ph}), 128.2 (C^{ph}), 127.0 (C^{ph}), 125.8 (C^{5-py}), 123.1 (C^{4-py}), 34.2 (NMe). MS (EI): *m/z* = 648 (100, [M]⁺), 633 (13, [M-Me]⁺), 324 (22, [M]²⁺). IR (KBr): ν (cm⁻¹) = 3056 (w), 2924 (m), 2854 (w), 1684

(m), 1584 (s), 1502 (w), 1472 (s), 1443 (m), 1384 (m), 1318 (w), 1261 (w), 1241 (w), 1154 (w), 1074 (m), 1025 (w), 992 (w), 957 (m), 915 (w), 844 (w), 791 (m), 774 (s), 720 (w), 696 (s), 651 (w).

II, L^4 : MeMgCl (3.0 M, 1.4 eq) was added slowly to a solution of **I** (1.0 eq) in THF (150 mL) at 0 °C. The reaction mixture was allowed to warm to rt and stirred overnight. Subsequently, the reaction was quenched with water. The organic layer was separated, the aqueous layer was extracted several times with dichloromethane and the combined organic layers were washed with brine and dried over MgSO₄. The solvent was evaporated under reduced pressure. L^4 and **II** were purified by column chromatography (silica gel, hexane/ethyl acetate 4:1 + 2 % NEt₃). *1,1-Bis(6-1-(ethoxymethyl)imidazole-2-yl)pyridine-2-yl)ethanol*, **II**: pale yellow powder, yield 78 % (2.8 g, 3.7 mmol). ¹H-NMR (CDCl₃): δ = 8.22 (dd, *J* = 7.6, 2.1 Hz, 2 H, H^{5-py}), 7.87-7.62 (m, 4 H, H^{3/4-py}), 7.60-7.37 (m, 14 H, H^{ph}), 7.27-7.07 (m, 6 H, H^{ph}), 6.59 (s, 1 H, OH), 5.75 (d, *J* = 9.8 Hz, 2 H, NCH₂O), 5.63 (d, *J* = 9.8 Hz, 2 H, NCH₂O), 3.27 (q, *J* = 7.0 Hz, 4 H, OCH₂Me), 2.07 (s, 3 H, C-(OH)-Me), 1.08 (t, *J* = 7.0 Hz, 6 H, OCH₂Me). ¹³C-NMR (CDCl₃): δ = 163.8 (C^{2-py}), 148.6 (C^{6-py}), 145.1 (C^{2-im}), 138.4 (C^{4-im}), 137.8 (C^{4-py}), 134.4 (C^{ph}), 132.2 (C^{5-im}), 131.5 (C^{ph}), 130.5 (C^{ph}), 129.1 (C^{ph}), 129.0 (C^{ph}), 127.2 (C^{ph}), 126.8 (C^{ph}), 122.0 (C^{5-py}), 119.8 (C^{3-py}), 77.1 (C-(OH)-Me), 74.0 (N-CH₂-O), 64.0 (O-CH₂-Me), 28.8 (C-(OH)-Me), 15.1 (-CH₂-Me). MS (ESI+, MeCN): *m/z* = 753.0 ([M+H]⁺), 775.0 ([M+Na]⁺). IR (KBr): ν (cm⁻¹) = 3367 (m, broad), 3056 (w), 2929 (w), 1570 (s), 1475 (s), 1442 (s), 1379 (m), 1326 (w), 1269 (w), 1200 (w), 1094 (s), 961 (m), 824 (m), 775 (s), 699 (s). *1,1-Bis(6-1-(methyl)imidazole-2-yl)pyridine-2-yl)ethanol*, L^4 : colourless powder, yield: 62 % (1.6 g, 2.3 mmol). ¹H-NMR (CDCl₃): δ = 8.20 (dd, *J* = 7.8, 0.9 Hz, 2 H, H^{5-py}), 7.77 (t, *J* = 7.8 Hz, 2 H, H^{4-py}), 7.61 (dd, *J* = 7.8, 0.9 Hz, 2 H, H^{3-py}), 7.56-7.44 (m, 10 H, H^{ph}), 7.42-7.38 (m, 4 H, H^{ph}), 7.25-7.14 (m, 6 H, H^{ph}), 5.93 (s, 1 H, OH), 3.83 (s, 6 H, NMe). ¹³C-NMR (CDCl₃): δ = 163.5 (C^{2-py}), 149.2 (C^{6-py}), 144.8 (C^{2-im}), 137.8 (C^{4-py}), 131.2 (C^{5-im}), 130.9 (C^{4-im}), 129.2 (C^{ph}), 128.9 (C^{ph}), 128.3 (C^{ph}), 127.1 (C^{ph}), 126.6 (C^{ph}), 122.3 (C^{3-py}), 119.4 (C^{5-py}), 77.1 (C-(OH)-Me), 34.4 (NCH₃), 28.7 (Me). MS (ESI, MeCN): *m/z* = 665.3 ([M+H]⁺), 687.3 ([M+Na]⁺). IR (KBr): ν (cm⁻¹) = 3203 (m, broad), 3059 (m), 3003 (m), 2982 (m), 2954 (m), 1897 (w), 1820 (w), 1603 (s), 1574 (s), 1502 (s), 1471 (s), 1385 (s), 1359 (s), 1322 (s), 1262 (s), 1221 (s), 1172 (s), 1131 (s), 1104 (s), 1089 (s), 1024 (m), 995 (m), 963 (s), 916 (s), 845 (s), 822 (s), 787 (s), 777 (s), 759 (s), 745 (s), 727 (s), 699 (s), 659 (m), 643 (m), 521 (m), 503 (m). C₄₄H₃₆N₆O calcd. C 79.5, H 5.46. N 12.4; found C 79.4, H 5.70, N 12.6.

L^2 : **II** (2.8 g, 3.7 mmol) was dissolved in a mixture of hydrochloric acid and water (1:1, 60 mL) and stirred at 60 °C for 4 h. The reaction mixture was neutralised with sodium hydroxide (35 % in water) and saturated aqueous sodium hydrocarbonate at 0 °C. The crude material was extracted several times with dichloromethane, washed with brine and dried over MgSO₄. L^2 was purified by column chromatography (silica gel, hexane/ethyl acetate 1:1 + 5 % NEt₃). *1,1-Bis(6-(4,5-diphenylimidazole-2-yl)pyridine-2-yl)ethanol*, L^2 : white powder, yield: 45 % (1.17 g, 1.7 mmol). ¹H-NMR (CDCl₃): δ = 13.09 (s, 2 H, NH), 7.99 (dd, *J* = 5.8, 3.0 Hz, 2 H, H^{5-py}), 7.92-7.83 (m, 4 H, H^{3/4-py}), 7.63-7.40 (m, 14 H, H^{ph}), 7.36-7.16 (m, 6 H, H^{ph}), 6.88 (s, 1 H, OH), 2.09 (s, 3 H, Me). ¹³C-NMR (CDCl₃): δ = 164.4 (C^{2-py}), 146.7 (C^{6-py}), 145.1 (C^{2-im}), 137.9 (C^{3/4-py}), 134.8 (C^{4/5-im}), 131.1 (C^{4/5-im}), 129.2 (C^{ph}), 128.7 (C^{ph}), 128.2 (C^{ph}), 126.9 (C^{ph}), 119.8 (C^{3/4-py}), 117.6 (C^{5-py}), 76.9 (C-(OH)-Me), 29.0 (Me). MS (ESI+, MeOH): *m/z* = 637.3 ([M+H]⁺), 659.3 ([M+Na]⁺). IR (KBr): ν (cm⁻¹) = 3167 (m, broad), 1591 (m), 1570 (s), 1476 (s), 1445 (s), 1258 (w), 1162 (m), 1073 (m), 767 (s), 695 (s). C₄₂H₃₂N₆O·H₂O calcd. C 77.0, H 5.23. N 12.8; found C 76.8, H 5.79, N 12.4.

The synthesis of the ligand L^5 was already reported,^[3] but we used a different procedure.

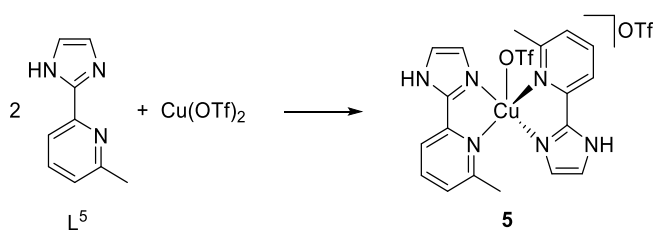


III: According to literature.^[4]

IV, 2-(1-(Ethoxymethyl)-1H-imidazol-2-yl)-6-methyl-pyridine: *n*-BuLi (1.6 M in hexane, 18.3 mL, 29.3 mmol, 1.03 eq.) was added to a solution of 1-ethoxymethyl-imidazole (3.57 g, 25.8 mmol, 1.00 eq.) in thf (10 mL) at $-78\text{ }^{\circ}\text{C}$. After 15 min of stirring, a solution of ZnCl_2 (10.6 g, 77.5 mmol, 2.7 eq) in thf (20 mL) was added and the reaction mixture allowed to warm to rt. A mixture of **III** (5.00 g, 25.8 mmol, 1.00 eq) and $\text{Pd}(\text{PPh}_3)_4$ (290 mg, 8 mol%) in thf (20 mL) was added and the reaction mixture stirred at $60\text{ }^{\circ}\text{C}$ for 5 h. The mixture was cooled to rt, poured into a solution of $\text{Na}_2\text{EDTA} \cdot 2\text{H}_2\text{O}$ (~3 eq.) in water, the pH was adjusted to 8 with aqueous Na_2CO_3 solution (10 %) and the aq. layer was extracted three times with dichloromethane. The combined organic extracts were washed with brine, dried over MgSO_4 and concentrated *in vacuo*. The crude product was purified by column chromatography on silica gel (hexane/EtOAc 1:1 + 3 % NEt_3) to give **IV** as a colourless oil (average yield 68 %, 4.27g). *Analytical data*: $^1\text{H-NMR}$ (CDCl_3): $\delta = 7.97$ (ddd, $J = 7.9, 1.1, 0.6$ Hz, 1H, $\text{H}^{3\text{-py}}$), 7.65 (t, $J = 7.8$ Hz, 1H, $\text{H}^{4\text{-py}}$), 7.21 (d, $J = 1.3$ Hz, 1H, $\text{H}^{5\text{-im}}$), 7.15 (d, $J = 1.3$ Hz, 1H, $\text{H}^{4\text{-im}}$), 7.09 (ddd, $J = 7.7, 1.0, 0.5$ Hz, 1H, $\text{H}^{5\text{-py}}$), 6.10 (s, 2H, $\text{N-CH}_2\text{-O}$), 3.53 (q, $J = 7.0$ Hz, 2H, $\text{O-CH}_2\text{-Me}$), 2.57 (s, 3H, Me) 1.15 (t, $J = 7.0$ Hz, 3H, $\text{O-CH}_2\text{-Me}$). $^{13}\text{C}\{^1\text{H}\}\text{-NMR}$ (CDCl_3): $\delta = 159.9$ ($\text{C}^{6\text{-py}}$), 149.8 ($\text{C}^{2\text{-py}}$), 145.1 ($\text{C}^{2\text{-im}}$), 137.2 ($\text{C}^{4\text{-py}}$), 129.0 ($\text{C}^{4\text{-im}}$), 122.3 ($\text{C}^{5\text{-py}}$), 122.3 ($\text{C}^{5\text{-im}}$), 120.1 ($\text{C}^{3\text{-py}}$), 77.1 ($\text{N-CH}_2\text{-O}$), 64.3 ($\text{O-CH}_2\text{-Me}$), 24.5 (Me), 15.1 ($\text{O-CH}_2\text{-Me}$). MS (ESI⁺ (MeCN)): $m/z = 218.1$ ($[\text{M}+\text{H}]^+$).

L⁵, 2-(1H-imidazol-2-yl)-6-methylpyridine: A solution of **IV** (4.27 g, 19.2 mmol, 1.00 eq.) in EtOH (15 mL) was treated with HCl (37 %, 15 mL) and stirred at $80\text{ }^{\circ}\text{C}$ for 5 h. Afterwards the pH was adjusted to 8 with an aqueous solution of Na_2CO_3 (10 %) and the aqueous layer was extracted with CH_2Cl_2 . The combined organic extracts were washed with an aqueous, saturated solution of NaCl, dried over MgSO_4 , filtered and concentrated *in vacuo*. The crude product was purified by column chromatography on silica gel with hexane/EtOAc 1:1 + 5% NEt_3 as eluent to give **L⁵** as colourless solid (2.06 g, 12.9 mmol, 38 %). *Additional analytical data*: $^1\text{H-NMR}$ (CDCl_3): $\delta = 10.85$ (s, 1H, NH), 7.98-7.95 (m, 1H, $\text{H}^{3\text{-py}}$), 7.65 (t, $J = 7.8$ Hz, 1H, $\text{H}^{4\text{-py}}$), 7.17 (d, $J = 7.0$ Hz, 2H, H^{im}), 7.12 – 6.98 (m, 2H, $\text{H}^{5\text{-py}}$), 2.52 (s, 3H, Me). $^{13}\text{C}\{^1\text{H}\}\text{-NMR}$ (CDCl_3): $\delta = 157.9$ ($\text{C}^{6\text{-py}}$), 148.0 ($\text{C}^{2\text{-py}}$), 146.7 ($\text{C}^{2\text{-im}}$), 137.5 ($\text{C}^{4\text{-py}}$), 130.5 ($\text{C}^{4/5\text{-im}}$), 122.9 ($\text{C}^{5\text{-py}}$), 117.0 ($\text{C}^{4/5\text{-py}}$), 116.9 ($\text{C}^{3\text{-py}}$), 24.4 (Me). MS (EI): m/z (%) = 159.1 (100, $[\text{M}]^+$), 144.1 (20, $[\text{M-Me}]^+$), 92.1 (15, $[\text{M-Im}]^+$).

Complex Synthesis



5: **L⁵** (150 mg, 0.92 mmol, 2.00 eq) and $\text{Cu}(\text{OTf})_2$ (166 mg, 0.46 mmol, 1.00 eq) were dissolved in methanol and stirred at rt for 2 h. Diethylether was added to the reaction mixture, the resulting precipitate collected and washed with thf three times. The green powder was dried *in vacuo* to give **5** (302 mg, 0.79 mmol, 86 %). A X-Ray diffraction experiment of single crystals confirmed the connectivity of the atoms but the quality of the data set does not allow for publication. The coordination of two equivalents of ligand was confirmed. These two ligands and the anion build up a distorted trigonal bipyramidal coordination sphere around the copper core. The change from the square pyramidal to the trigonal bipyramidal coordination sphere around the copper(II) ion is caused by steric hindrance between the methyl groups in 6-position of the pyridinyl moieties. *Analytical data*: MS (ESI⁺ (MeOH)): $m/z = 530.0$ ($[\text{M-OTf}]^+$), 380.1 ($[\text{M-H-2OTf}]^+$). HR-MS: calculated $\text{C}_{19}\text{H}_{18}\text{CuF}_3\text{N}_6\text{O}_3\text{S}$: 530.0404, found: 530.0408. $\text{C}_{20}\text{H}_{18}\text{CuF}_6\text{N}_6\text{O}_6\text{S}_2 \cdot 2\text{H}_2\text{O}$ calcd.: C 33.6, H 3.10, N 11.7, S 8.95; found C 34.0, H 3.10, N 11.7, S

9.45, IR (KBr): ν (cm⁻¹) = 3651 (m), 3214 (m), 3126 (w), 2948 (w), 1627 (m), 1569 (m), 1482 (s), 1447 (w), 1410 (w), 1294 (s), 1246 (vs)*, 1166 (s)*, 1105 (m), 1038 (s)*, 973 (m), 878 (m), 854 (m), 804 (w), 779 (m), 746 (m), 713 (m), 688 (m). * = triflate anion^[5]

2) Molecular Structure

a) X-ray Crystallography

X-ray data were collected with a *STOE IPDS II* diffractometer (graphite monochromated Mo-K α radiation, $\lambda = 0.71073$ Å) by use of ω scans at -140 °C. The structure was solved by direct methods and refined on F^2 using all reflections with SHELX-2013.^[6] Most non-hydrogen atoms were refined anisotropically. Most hydrogen atoms were placed in calculated positions and assigned to an isotropic displacement parameter of 1.2 / 1.5 U_{eq} (C). Face-indexed absorption corrections were performed numerically with the programme X-RED.^[7] CCDC-1442849, CCDC-1442850, CCDC-1442851, and CCDC-1430302 contain the supplementary crystallographic data for this paper. The data can be obtained free of charge from *The Cambridge Crystallographic Data Centre* via www.ccdc.cam.ac.uk/data_request/cif.

Table S 1. Crystal data and refinement details for **2bH₃**, **3bH₁**, **4bH₁**, and **3a**.

compound	2bH₃	3bH₁	4bH₁	3a
empirical formula	C ₄₅ H ₃₈ Cu ₂ N ₆ O ₅	C _{23.50} H _{22.50} Cu ₂ N ₆ O ₉	C ₄₇ H ₃₈ Cu ₂ N ₆ O ₇	C ₂₃ H ₃₂ Br ₂ CuN ₆ O ₄
formula weight	869.89	660.05	925.91	679.90
<i>T</i> [K]	133(2)	133(2)	133(2)	133(2)
crystal size [mm ³]	0.500×0.200×0.160	0.35×0.2×0.09	0.246×0.23×0.086	0.500×0.500×0.070
crystal system	orthorhombic	triclinic	triclinic	monoclinic
space group	<i>P</i> 2 ₁ 2 ₁ 2 ₁	<i>P</i> -1	<i>P</i> -1	<i>P</i> 2 ₁ / <i>n</i>
<i>a</i> [Å]	15.2115(3)	8.8934(18)	11.231(2)	13.241(3)
<i>b</i> [Å]	16.7551(4)	10.975(2)	12.002(2)	13.767(3)
<i>c</i> [Å]	19.9050(4)	13.212(3)	15.218(3)	29.787(6)
α [°]	90	79.75(3)	98.67(3)	90
β [°]	90	80.08(3)	97.62(3)	94.56(3)
γ [°]	90	84.89(3)	95.17(3)	90
<i>V</i> [Å ³]	5073.19(19)	1247.6(5)	1997.3(7)	5412.4(19)
<i>Z</i>	4	2	2	8
ρ [g/cm ³]	1.139	1.757	1.540	1.669
<i>F</i> (000)	1792	671	952	2744
μ [mm ⁻¹]	0.882	1.772	1.128	3.800
<i>T</i> _{min} / <i>T</i> _{max}	0.6961 / 0.9033	0.6297 / 0.8408	0.7367 / 0.8794	0.2825 / 0.5520
θ -range [°]	1.589 - 25.679	1.587 - 26.732	1.369 - 26.742	1.372 - 25.639
<i>hkl</i> -range	±18, ±20, -24 - 23	±11, ±13, -14 - 16	±14, ±15, -19 - 18	±16, ±16, ±36
measured refl.	59629	13815	25763	59871
unique refl. [<i>R</i> _{int}]	9580 [0.0831]	5294 [0.0425]	8463 [0.0795]	10199 [0.1472]
observed refl. (<i>I</i> > 2 σ (<i>I</i>))	8583	4522	6357	8263
data / restraints / param.	9580 / 3 / 528	10199 / 0 / 669	5294 / 26 / 390	8463 / 3 / 571
goodness-of-fit (F^2)	0.987	1.096	1.032	0.943
<i>R</i> 1, <i>wR</i> 2 (<i>I</i> > 2 σ (<i>I</i>))	0.0358, 0.0835	0.0624, 0.1585	0.0416, 0.1088	0.0421, 0.1009
<i>R</i> 1, <i>wR</i> 2 (all data)	0.0410, 0.0853	0.0773, 0.1671	0.0497, 0.1130	0.0610, 0.1071
resid. el. dens. [e/Å ³]	-0.294 / 0.362	-1.341 / 1.376	-1.095 / 0.517	-0.627 / 0.903

Table S 2. Selected bond lengths [\AA] and angles [$^\circ$] for **3a**·3MeOH.

Atoms	3a ·3MeOH		3a 3MeOH
Cu(1)–N(1)	1.973(5)	Cu(2)–N(14)	1.971(5)
Cu(1)–N(4)	1.984(5)	Cu(2)–N(11)	1.982(5)
Cu(1)–N(6)	2.022(5)	Cu(2)–N(13)	2.033(5)
Cu(1)–N(3)	2.045(5)	Cu(2)–N(16)	2.038(5)
Cu(1)–Br(1)	2.6748(9)	Cu(2)–Br(2)	2.6749(9)
Cu(1)–O(21)	2.826(4)	Cu(1)–O(31)	2.978(4)
N(1)–Cu(1)–N(4)	99.53(19)	N(14)–Cu(2)–N(11)	99.88(19)
N(1)–Cu(1)–N(6)	163.47(16)	N(14)–Cu(2)–N(13)	162.61(17)
N(4)–Cu(1)–N(6)	82.26(19)	N(11)–Cu(2)–N(13)	82.21(19)
N(1)–Cu(1)–N(3)	82.01(19)	N(14)–Cu(2)–N(16)	81.41(19)
N(4)–Cu(1)–N(3)	161.97(16)	N(11)–Cu(2)–N(16)	158.32(17)
N(6)–Cu(1)–N(3)	91.30(18)	N(13)–Cu(2)–N(16)	90.36(18)
N(1)–Cu(1)–Br(1)	95.59(11)	N(14)–Cu(2)–Br(2)	94.12(12)
N(4)–Cu(1)–Br(1)	94.66(12)	N(11)–Cu(2)–Br(2)	92.86(12)
N(6)–Cu(1)–Br(1)	100.66(12)	N(13)–Cu(2)–Br(2)	103.04(11)
N(3)–Cu(1)–Br(1)	103.09(11)	N(16)–Cu(2)–Br(2)	108.69(12)

Table S 3. Selected bond lengths [\AA] and angles [$^\circ$] for **2bH₃**, **3bH₁**, and **4bH₁**.

Atoms	2bH₃	3bH₁	4bH₁
Cu1–O1	1.968(2)	1.985(2)	1.970(2)
Cu1–O2	1.934(3)	1.964(2)	1.948(2)
Cu1–N1	1.940(3)	1.954(3)	1.958(2)
Cu1–N2	2.016(3)	2.020(3)	2.056(2)
Cu1–O4	2.293(3)	2.152(2)	2.208(2)
Cu2–O1	1.968(2)	1.967(2)	1.9589(19)
Cu2–N4	1.932(3)	1.942(2)	1.939(2)
Cu2–O3	1.920(3)	1.933(2)	1.950(2)
Cu2–N5	1.991(3)	2.005(3)	2.029(2)
Cu2–O6		2.354(12)	2.220(3)
Cu2–O5	2.270(3)		

b) Hydrogen Bond Network

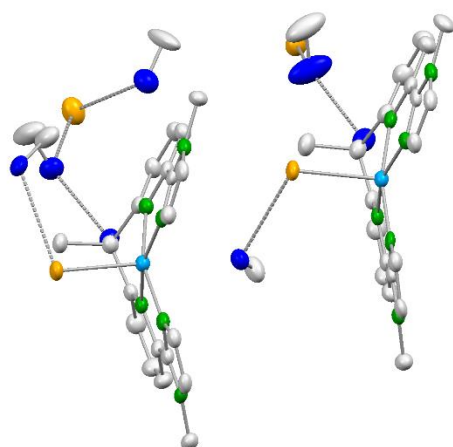


Figure S 1. Hydrogen bond network in the solid state structure of **3a**·3MeOH; bromine atoms are depicted in yellow, nitrogen atoms in green, oxygen atoms in blue, carbon atoms in grey and copper atoms in light blue.

Table S 4. Hydrogen bonds for **3a**-3MeOH [\AA] and [$^\circ$].

D-H...A	d(D-H)	d(H...A)	d(D...A)	$\angle(\text{DHA})$
O(1)-H(1)...O(43)	0.84	1.87	2.680(8)	163.0
O(21)-H(21)...Br(2)#1	0.84	2.42	3.248(5)	171.0
O(31)-H(31)...Br(1)#2	0.84	2.52	3.324(5)	161.3
O(41)-H(41)...Br(3)	0.84	2.45	3.290(6)	173.0
O(42)-H(42)...Br(3)	0.84	2.39	3.202(5)	162.4
O(43)-H(43)...Br(4)	0.84	2.34	3.144(6)	159.5
O(44)-H(44)...Br(4)	0.84	2.38	3.216(7)	172.7

Symmetry transformations used to generate equivalent atoms: #1 $-x+1, -y+1, -z+1$ #2 $-x+2, -y+1, -z+1$.

3) pK_a -Determinations of the Ligands

a) Potentiometric Determinations of the pK_a of L^2 and L^3

Triplicate titrations of the free ligands (L^2 : 195-259; L^3 : 289-436 points) were carried out. The ligand concentration was 2.0 mM in all titrations. HYPERQUAD2008^[8] computer programmes that use non-linear least square methods^[9] were applied to calculate the stability constants. The distribution curves of the protonated species of L^2 and L^3 , respectively, as a function of pH were calculated using the HySS2009 programme.^[10] The results of the fitting procedure are shown in Table S 5.

Table S 5. Overall protonation constants of the ligands L^2 and L^3 stability constants $\log \beta$ and proton dissociation constants pK_a at 25.0(2) $^\circ\text{C}$. Solvent: MeOH/water 80/20 by weight, $I = 0.1 \text{ M KCl}$. Standard deviations of calculated values are given in parentheses, charges are omitted for clarity.

ligand	L^2	L^3
$\log \beta$ (HL)	4.45(5)	5.31(9)
$\log \beta$ (H_2L)	7.70(4)	9.63(8)
$\log \beta$ (H_3L)	9.44(5)	12.08(9)
pK_a (HL)	4.45	5.31
pK_a (H_2L)	3.25	4.32
pK_a (H_3L)	1.74	2.45

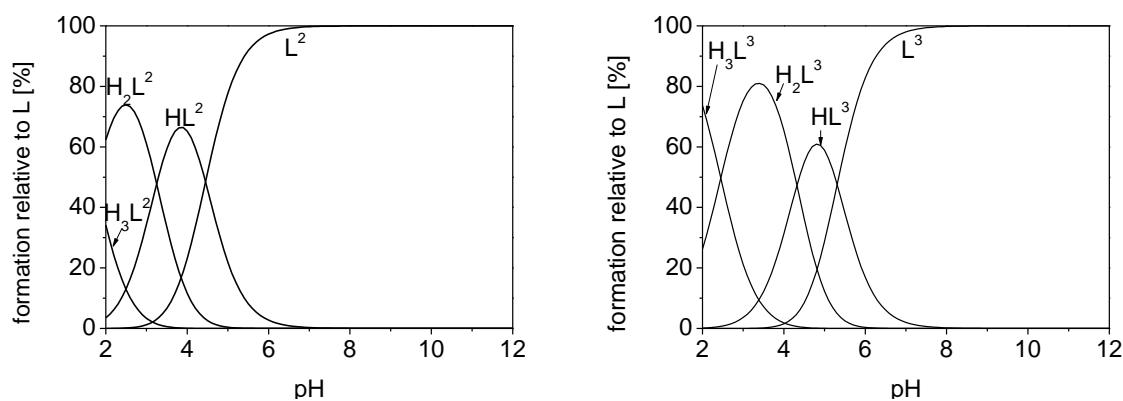


Figure S 2. Species distribution of the L^2 - (left) and L^3 -system (right). $[L] = 2.0 \text{ mM}$. Solvent: MeOH/water 80/20 by weight; $I = 0.1 \text{ M KCl}$. Charges are omitted for clarity.

b) Spectrophotometric Titrations for the Determination of the pK_a of L^4

L^4 was dissolved in 0.1 M KCl solution (MeOH/water 80/20 by weight). The pH was adjusted to $pH \sim 2$ by addition of 0.1 M HCl. Aliquots of KOH (dissolved in MeOH/water 80/20 by weight) were added. The data were fitted by using *Spectfit*TM.^[11] The model and input parameters are shown in Table S 6.

Table S 6 Model and input parameters for L^4 , values marked with asterisks have been obtained by fitting. Charges are omitted for clarity.

species [$M_x(L)_yH_z$]	coloured	spectra fixed	value fixed	parameter	error
0 1 0 = L^4	True	False*	True	0.0	0.0
0 1 1 = HL^4	True	False*	False	6.46	0.07
0 1 2 = H_2L^4	True	False*	False	9.82	0.08

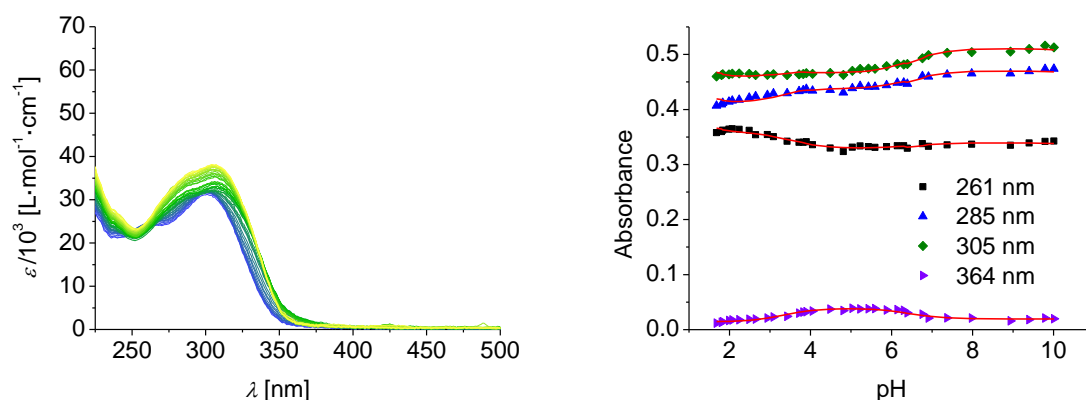


Figure S 3. Left: pH-dependent UV/Vis spectra L^4 in MeOH/water (80/20 by weight), right: trend of the absorbance at four different wavelengths (261, 285, 305 and 364 nm), the red lines represent the fits; $I = 0.1$ M KCl, $[L^4] = 15 \mu M$.

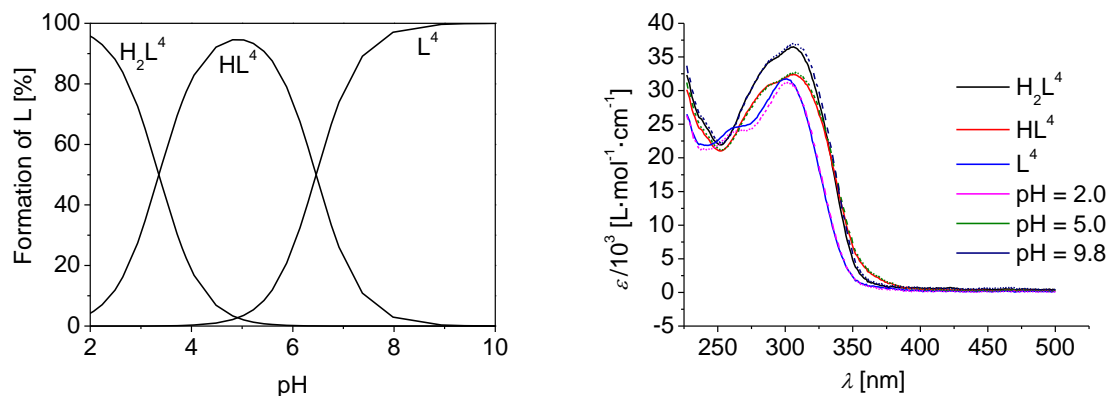


Figure S 4. Left: Species distribution of the L^4 -system in MeOH/water (80/20 by weight), right: simulated and measured spectra of L^4 at different protonation states. $I = 0.1$ M KCl, $[L^4] = 15 \mu M$. Charges are omitted for clarity.

4) Spectrophotometric Titrations

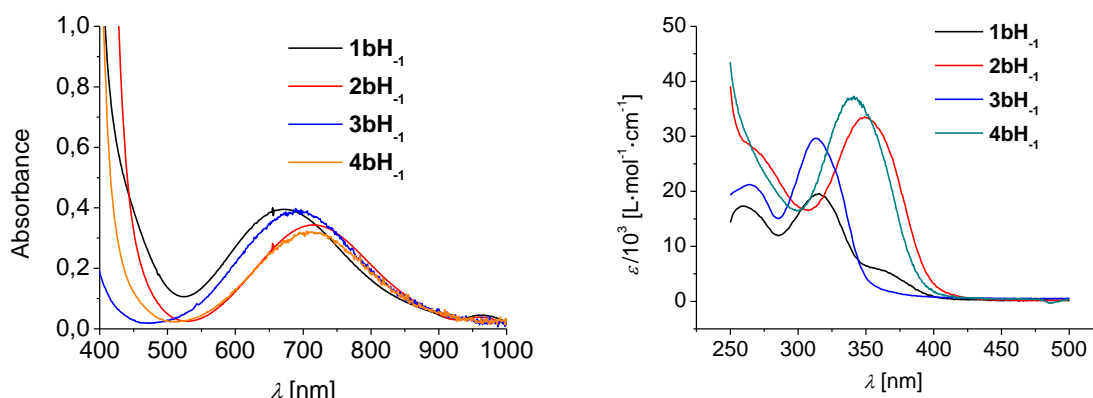


Figure S 5. Representative Vis spectra (left) and UV spectra (right) of the dinuclear copper(II) complexes **1bH₋₁**, **2bH₋₁**, **3bH₋₁**, and **4bH₋₁** in MeOH/water (80/20 by weight). $I = 0.1 \text{ M NaOAc}$.

Table S 7. Overview of the UV bands of the $[\text{Cu}_2\text{LH}_{-1}]^{3+}$ complexes in MeOH/water.

λ ($\epsilon/10^3$) [nm ($\text{M}^{-1}\text{cm}^{-1}$)]	1bH₋₁	2bH₋₁	3bH₋₁	4bH₋₁
ILCT	263 (17)	269(28)	265 (21)	
ILCT	313(20)	350 (33)	314 (30)	335(32)
ILCT	356 (6)			

a) Species Distributions of the $\text{L}^{1-4}\text{-Cu(II)}$ Systems in MeOH/Water

The complexes were dissolved in 0.1 M NaOAc solutions (MeOH/water 80/20 by weight). The pH was adjusted to $\text{pH} \sim 12$ by addition of KOH. Aliquots of HOAc (dissolved in MeOH/water 80/20 by weight) were added. The pH values were measured by a combined glass electrode (Metrohm 6.0234.100) filled with 0.1 M NaCl solution in MeOH/water (80/20 by weight). The data were fitted by using *Spectfit*TM.^[11] The model and input parameters are shown in Table S 8-S 11.

i) Complex **3bH₋₁**

Table S 8. Model and input parameters for the CuL^3 -system, values marked with asterisks have been obtained by fitting. Charges are omitted for clarity.

Species [$\text{M}_x(\text{L})_y\text{H}_z$]	coloured	spectra fixed	value fixed	parameter	error
1 0 0 = Cu	False	False	True	0.0	0.0
0 1 0 = L ³	True	True	True	0.0	0.0
0 1 1 = HL ³	True	True	True	5.31	0.0
0 1 2 = H ₂ L ³	True	True	True	9.63	0.0
1 1 0 = 3a	True	True	False*	7.17*	0.08*
2 1 -1 = 3bH₋₁	True	False*	False*	6.84*	0.10*
2 1 -2 = 3bH₋₂	True	False*	False*	-4.60 *	0.14*

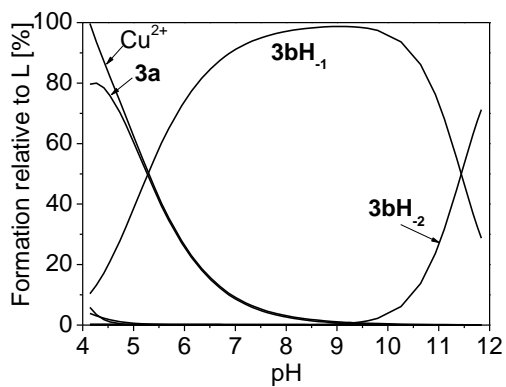


Figure S 6. Species distribution of the CuL^3 -system in dependence of pH ($c = 25 \mu\text{M}$); conditions: MeOH/water (80/20 by weight), $I = 0.1 \text{ M NaOAc}$.

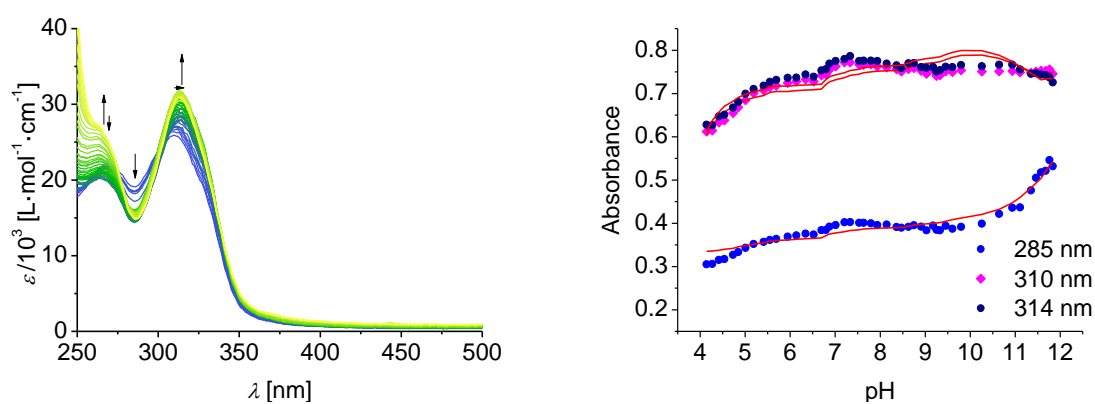


Figure S 7. Left: pH-dependent UV/Vis spectra of 3bH_{-1} in MeOH/water (80/20 by weight), right: trend of the absorbance at three different wavelengths (285, 310, and 314 nm), the red lines represent the fits; $I = 0.1 \text{ M NaOAc}$, $[3\text{bH}_{-1}] = 25 \mu\text{M}$.

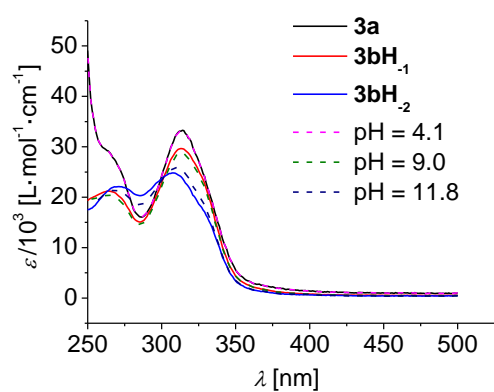


Figure S 8. Simulated and measured spectra of the CuL^3 -system at different protonation states. Charges are omitted for clarity. $I = 0.1 \text{ M NaOAc}$, $[3\text{bH}_{-1}] = 25 \mu\text{M}$.

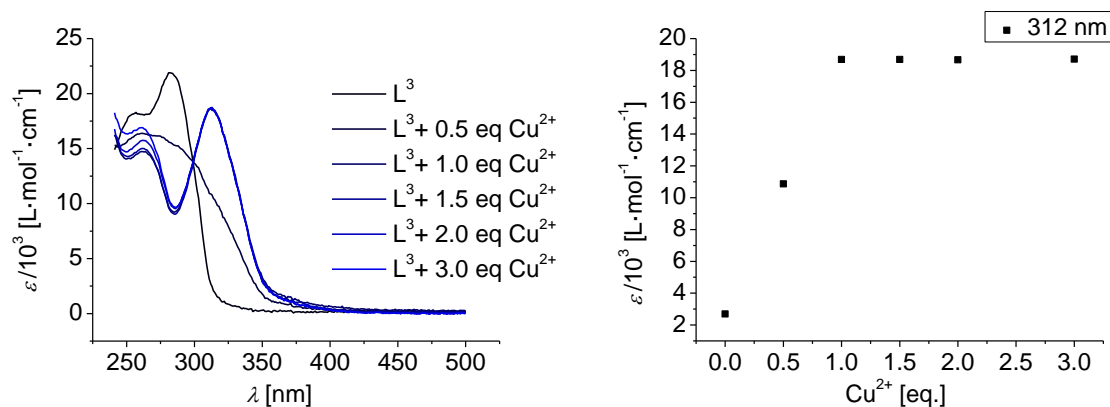


Figure S 9. Left: UV/Vis spectra of L^3 upon adding Cu^{2+} ions in MeOH/water (80/20 by weight); right: trend of the absorbance at 312 nm; $I = 0.1$ M NaOAc, $pH = 3.9$, $[L^3] = 25$ μM .

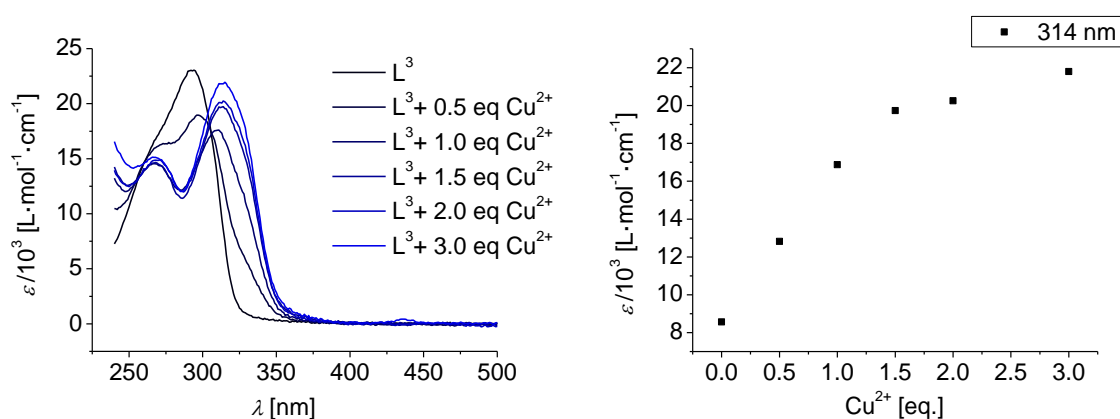


Figure S 10. Left: UV/Vis spectra of L^3 upon adding Cu^{2+} ions in MeOH/water (80/20 by weight); right: trend of the absorbance at 314 nm; $I = 0.1$ M NaOAc, $pH = 10.7$, $[L^3] = 25$ μM .

ii) Complex **4bH₁**

Table S 9. Model and input parameters for the CuL^4 -system, values marked with asterisks have been obtained by fitting. Charges are omitted for clarity.

Species [$M_x(L)_yH_z$]	coloured	spectra fixed	value fixed	parameter	error
1 0 0 = Cu	False	False	True	0.0	0.0
0 1 0 = L^4	True	True	True	0.0	0.0
0 1 1 = HL^4	True	True	True	6.46	0.0
0 1 2 = H_2L^4	True	True	True	9.80	0.0
2 1 0 = Cu_2L^4	True	False	False*	13.51 ^{§*}	0.14 [§]
2 1 -1 = 4bH₁	True	False	False*	5.86 ^{§*}	0.05/0.10 [§]
2 1 -2 = 4bH₂	True	False	False*	-3.40 ^{§*}	0.12 [§]

[§] We could not reach convergence, when all three values were fitted at once. Therefore we fitted the values iterative, that is the first two values were fitted while the third one was fixed, and then the other way around (i.e. the first value was fixed and the other two were fitted). The procedure was repeated till all values did not change any further upon fitting.

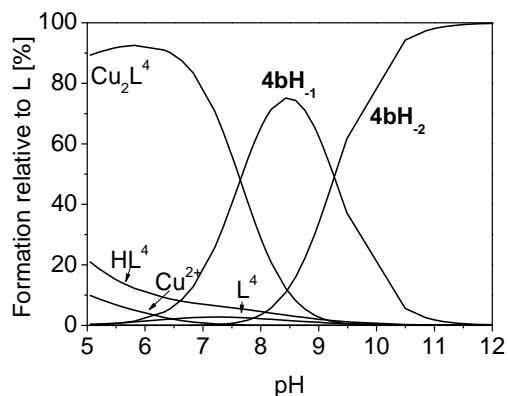


Figure S 11. Species distribution of the CuL^4 -system in dependence of pH ($c = 15 \mu\text{M}$); conditions: MeOH/water (80/20 by weight), $I = 0.1 \text{ M NaOAc}$. Charges are omitted for clarity.

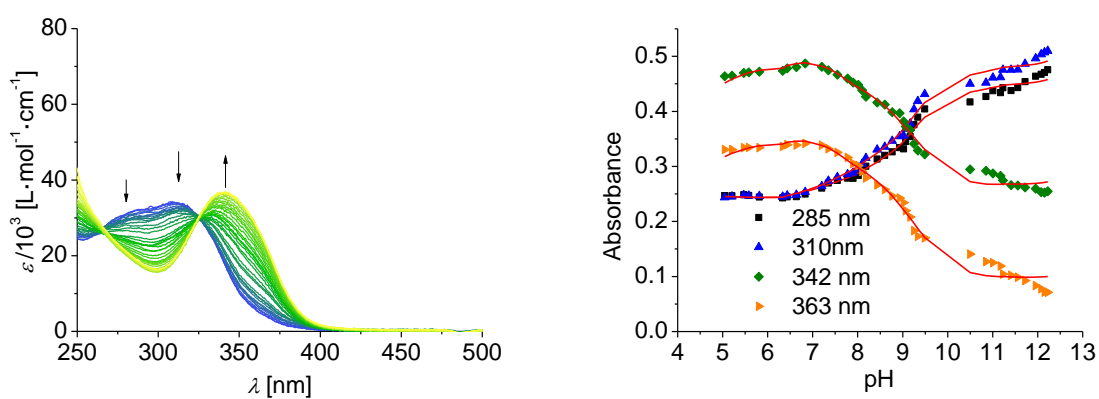


Figure S 12. Left: pH-dependent UV/Vis spectra of 4bH_{-1} in MeOH/water (80/20 by weight), right: trend of the absorbance at four different wavelengths (285, 310, 342, and 363 nm), the red lines represent the fits; $I = 0.1 \text{ M NaOAc}$, $[4\text{bH}_{-1}] = 15 \mu\text{M}$.

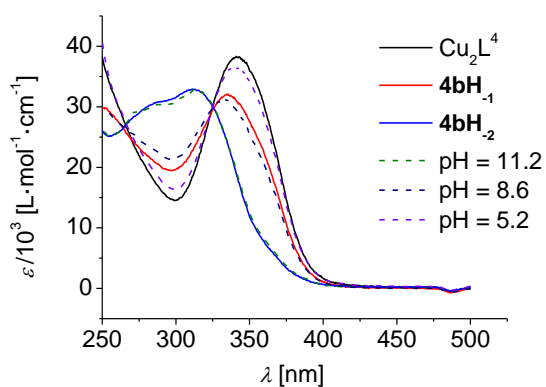


Figure S 13. Simulated and measured spectra of the CuL^4 -system at different protonation states. Charges are omitted for clarity. $I = 0.1 \text{ M NaOAc}$, $[4\text{bH}_{-1}] = 15 \mu\text{M}$.

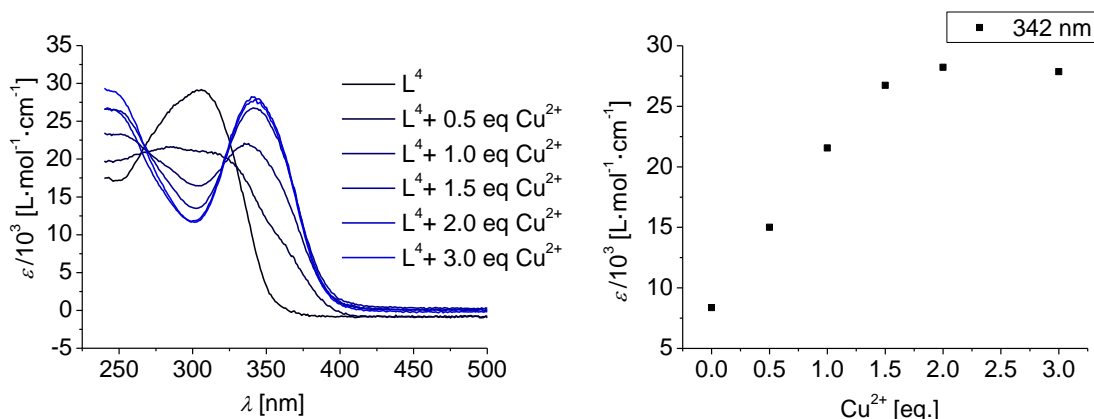


Figure S 14. Left: UV/Vis spectra of L^4 upon adding Cu^{2+} ions in MeOH/water (80/20 by weight); right: trend of the absorbance at 342 nm; $I = 0.1$ M NaOAc, $pH = 4.4$, $[L^4] = 15$ μM .

iii) Complex **1bH₃**

Table S 10. Model and input parameters for the CuL^1 -system, values marked with asterisks have been obtained by fitting. Charges are omitted for clarity.

Species [$M_x(L)_yH_z$]	coloured	spectra fixed	value fixed	parameter	error
1 0 0 = Cu	False	False	True	0.0	0.0
0 1 0 = L^1	True	True	True	0.0	0.0
0 1 1 = HL^1	True	True	True	5.24	0.0
0 1 2 = H_2L^1	True	True	True	9.31	0.0
1 1 0 = 1a	True	True	False*	7.67*	0.50*
2 1 -1 = 1bH₁	True	False*	False*	6.35*	0.51*
2 1 -2 = 1bH₂	True	False*	False*	-1.41*	0.51*
2 1 -3 = 1bH₃	True	True	False*	-11.96*	0.51*

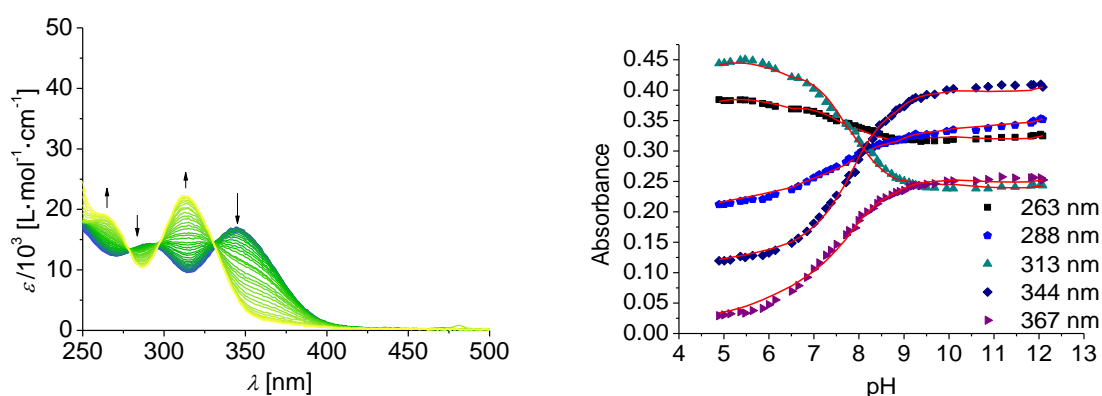


Figure S 15. Left: pH-dependent UV/Vis spectra of **1bH₃** in MeOH/water (80/20 by weight), right: trend of the absorbance at five different wavelengths (263, 288, 313, 344, and 367 nm), the red lines represent the fits; $I = 0.1$ M NaOAc, $[1bH_3] = 25$ μM .

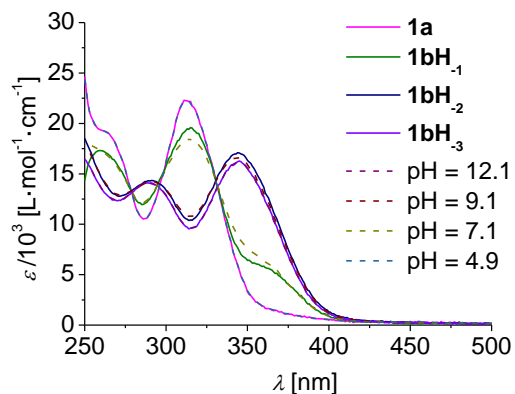


Figure S 16 Simulated and measured spectra of the CuL^1 -system at different protonation states. Charges omitted for clarity. $l = 0.1 \text{ M NaOAc}$, $[\mathbf{1bH}_{-3}] = 25 \mu\text{M}$.

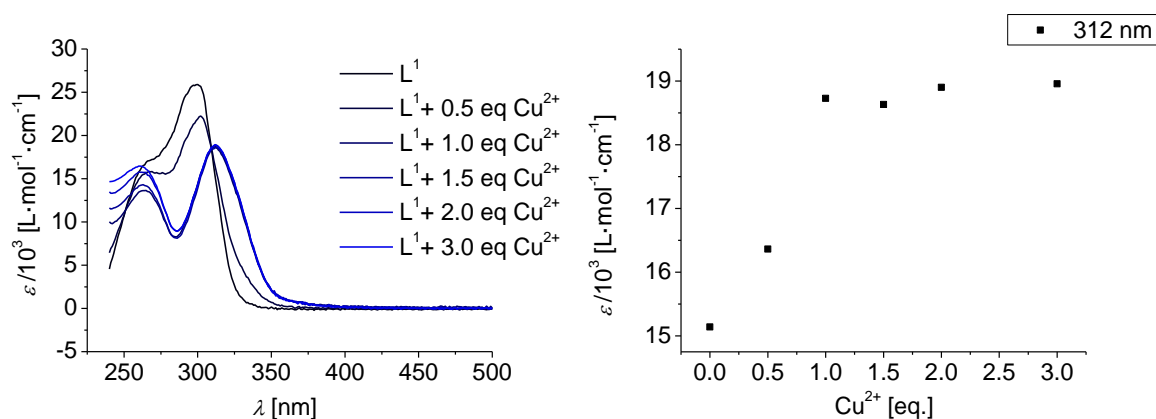


Figure S 17. Left: UV/Vis spectra of L^1 upon adding Cu^{2+} ions in MeOH/water (80/20 by weight); right: trend of the absorbance at 312 nm; $l = 0.1 \text{ M NaOAc}$, $\text{pH} = 4.5$, $[L^1] = 25 \mu\text{M}$.

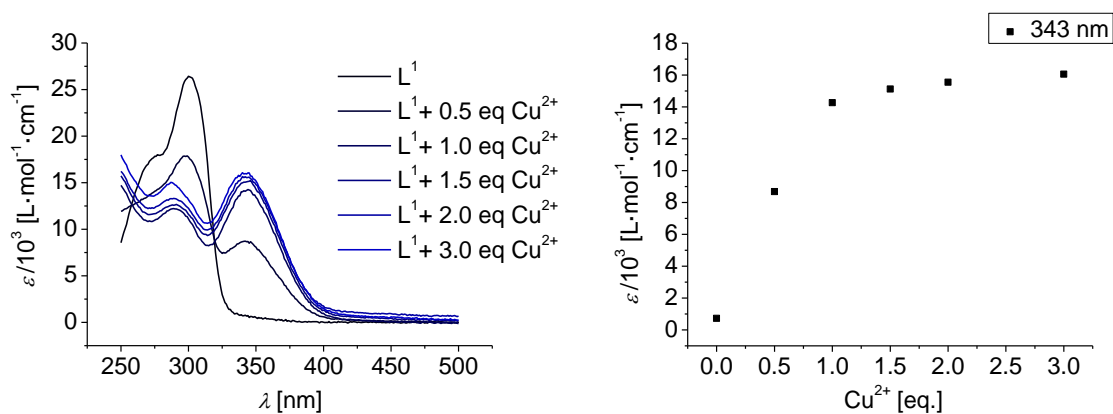


Figure S 18. Left: UV/Vis spectra of L^1 upon adding Cu^{2+} ions in MeOH/water (80/20 by weight); right: trend of the absorbance at 343 nm; $l = 0.1 \text{ M NaOAc}$, $\text{pH} = 10.7$, $[L^1] = 25 \mu\text{M}$.

iv) Complex **2bH₃**

Table S 11. Model and input parameters for the CuL²-system, values marked with asterisks have been obtained by fitting. Charges are omitted for clarity.

Species [M _x (L) _y H _z]	coloured	spectra fixed	value fixed	parameter	error
1 0 0 = Cu	False	False	True	0.0	0.0
0 1 0 = L ²	True	True	True	0.0	0.0
0 1 0 = HL ²	True	True	True	4.45	0.0
0 1 1 = H ₂ L ²	True	True	True	7.70	0.0
1 1 0 = L ² Cu	True	False*	False*	6.42*	0.26*
2 1 -1 = 2bH₁	True	True	False*	7.00*	0.37*
2 1 -2 = 2bH₂	True	True	False*	0.23*	0.36*
2 1 -3 = 2bH₃	True	False*	False*	-9.42*	0.37*

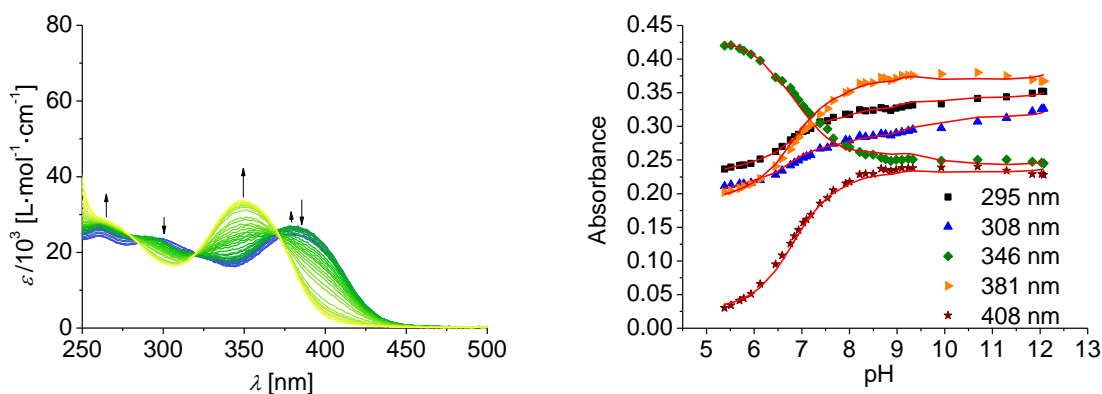


Figure S 19. Left: pH-dependent UV/Vis spectra of **2bH₃** in MeOH/water (80/20 by weight), right: trend of the absorbance at five different wavelengths (295, 308, 346, 381, and 408 nm), the red lines represent the fits; $I = 0.1$ M NaOAc, $[2bH_3] = 15$ μ M.

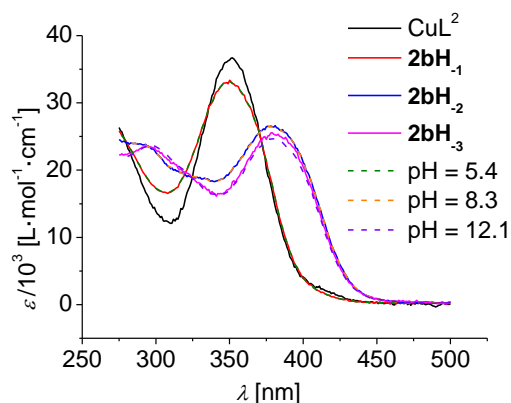


Figure S 20. Simulated and measured spectra of the CuL²-system at different protonation states. Charges are omitted for clarity. $I = 0.1$ M NaOAc, $[2bH_3] = 15$ μ M.

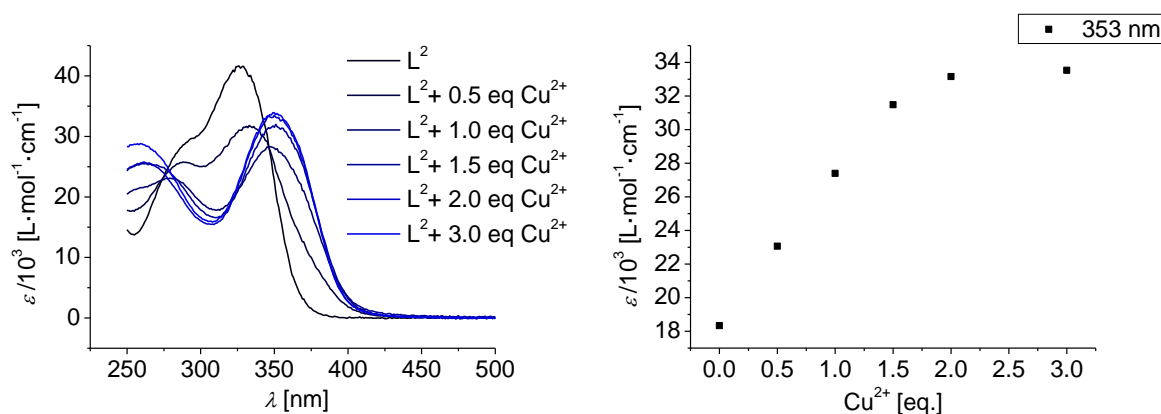


Figure S 21. Left: UV/Vis spectra of L^2 upon adding Cu^{2+} ions in MeOH/water (80/20 by weight); right: trend of the absorbance at 353 nm; $I = 0.1 \text{ M NaOAc}$, $\text{pH} = 4.5$, $[L^2] = 15 \mu\text{M}$.

b) Species Distributions in Water

i) Employing L^1

The ligand was dissolved in 0.1 M aqueous phosphoric acid solution and the solution's pH was adjusted to $\text{pH} \sim 2$ with KOH solution. Aliquots of KOH solution were added. The data were fitted by using *Spectfit*TM.^[11] The model and input parameters are shown in Table S 12.

Table S 12. Model and input parameters for L^1 , values marked with asterisks have been obtained by fitting. Charges are omitted for clarity.

species [$\text{M}_x(\text{L})_y\text{H}_z$]	coloured	spectra fixed	value fixed	parameter	error
0 1 0 = $L^1\text{H}_{-1}$	True	False*	True	0.0	0.0
0 1 1 = L^1	True	False*	False	11.241*	0.04275*
0 1 2 = HL^1	True	False*	False	16.778*	0.05302*
0 1 3 = H_2L^1	True	False*	False	20.357*	0.1077*

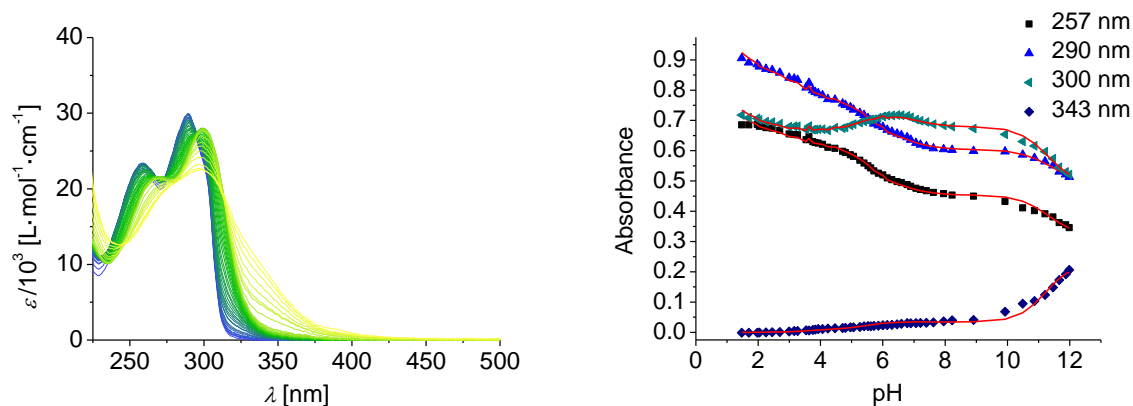


Figure S 22. Left: pH-dependent UV/Vis spectra L^1 in water, right: trend of the absorbance at four different wavelength (257, 290, 300 and 343 nm; right), the red lines represent the fits; $I = 0.1 \text{ M PO}_4^{3-}$, $[L^1] = 31 \mu\text{M}$.

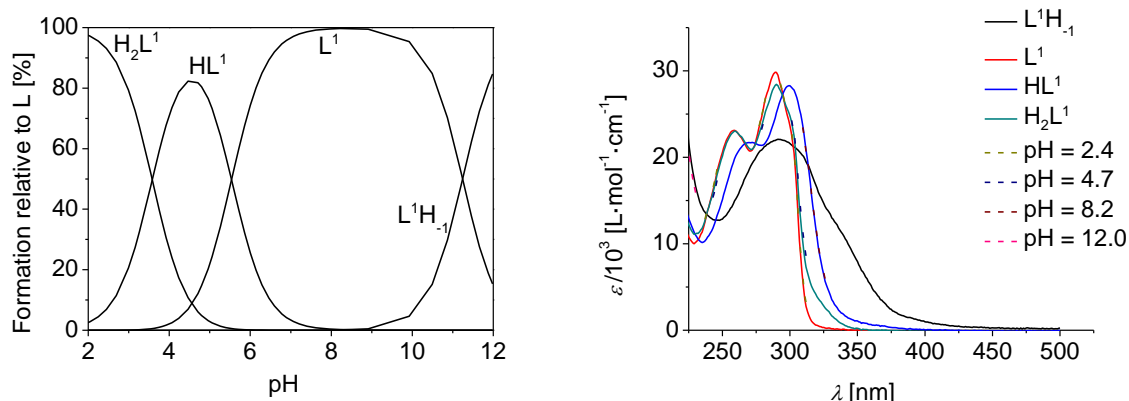


Figure S 23. Left: Species distribution of the L^1 -system in water; right: simulated and measured spectra of L^1 at different protonation states. $I = 0.1 \text{ M PO}_4^{3-}$, $[L^1] = 31 \mu\text{M}$. Charges are omitted for clarity.

L^1 was dissolved in 0.1 M aqueous phosphoric acid solution and the solution's pH was adjusted to pH = 2.5 with KOH solution. Aliquots of a $\text{Cu}(\text{OTf})_2$ solution were added, $c = 399 \mu\text{M}$. The data were fitted by using *Spectfit*TM.^[11] The model and input parameters are shown in Table S 13.

Table S 13. Model and input parameters for the L^1 - Cu^{2+} -titration, values marked with asterisks have been obtained by fitting. Charges are omitted for clarity.

species [$M_x(L)_yH_z$]	coloured	spectra fixed	value fixed	parameter	error
100 = Cu	False	False	True	0.0	0.0
0 1 0 = L^1H_{-1}	True	True ^[a]	True	0.0	0.0
0 1 1 = L^1	True	True ^[a]	True	11.24	0.0
0 1 2 = HL^1	True	True ^[a]	True	16.78	0.0
0 1 3 = H_2L^1	True	False*	True	20.36	0.0
1 1 1 = 1a	True	True	False	23.308*	0.2176*

^[a]The calculated spectra from the ligand fit have been used as fixed spectra.

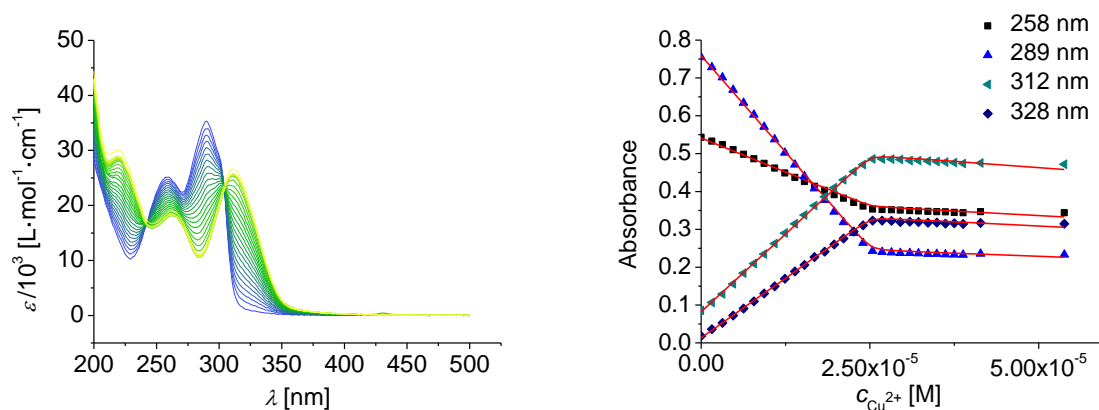


Figure S 24. Left: UV/Vis spectra of L^1 upon adding Cu^{2+} ions in water; right: trend of the absorbance at four different wavelength (258, 289, 312, and 328 nm), the red lines represent the fits; $I = 0.1 \text{ M PO}_4^{3-}$, pH = 2.5, $[L^1] = 26 \mu\text{M}$.

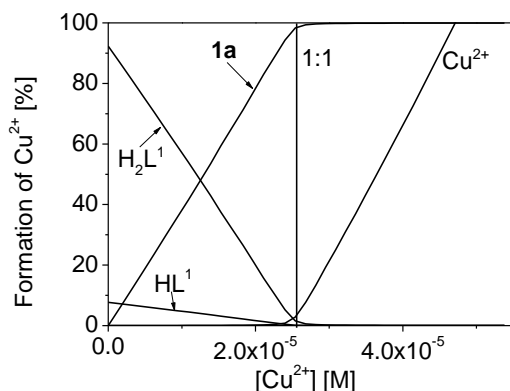


Figure S 25. Species distribution of L^1 upon adding Cu^{2+} ions in water; $I = 0.1 \text{ M } PO_4^{3-}$, $pH = 2.5$, $[L^1] = 26 \mu\text{M}$. Charges are omitted for clarity.

ii) Employing L^5

The ligand was dissolved in 0.1 M aqueous phosphoric acid solution and the solution's pH was adjusted to $pH \sim 1.7$ with KOH solution. Aliquots of KOH solution were added. The data were fitted by using *Spectfit*TM.^[11] The model and input parameters are shown in Table S 14. We also employed a model with 2 protonation steps, but the fits were not reasonable. This in line with literature reports for similar ligands, in which also only one protonation step has been observed in the pH range of 2-11 (cf. 2,2'-bisimidazol $pK_{a,1} = 5.185$, $pK_{a,2} < 1$; 2,2'-bipyridine $pK_{a,1} = 7.22$).^[12]

Table S 14. Model and input parameters for L^5 , values marked with an asterisk have been obtained by fitting. Charges are omitted for clarity.

species [$M_x(L)_yH_z$]	coloured	spectra fixed	value fixed	parameter	error
0 1 0 = L^5	True	False*	True	0.0	0.0
0 1 1 = HL^5	True	False*	False	5.75118*	0.03597*

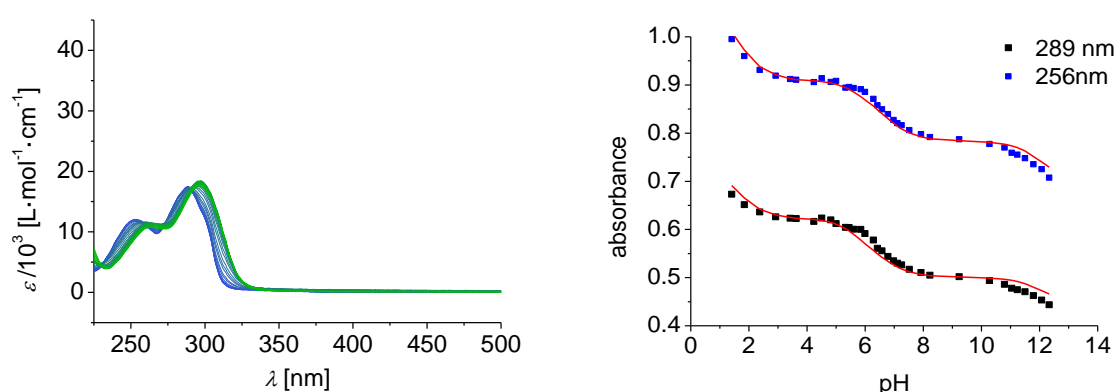


Figure S 26. Left: pH-dependent UV/Vis spectra L^5 in water; right: trend of the absorbance at two different wavelength (256 nm and 289 nm), the red lines represent the fits; $I = 0.1 \text{ M } PO_4^{3-}$, $[L^5] = 30 \mu\text{M}$.

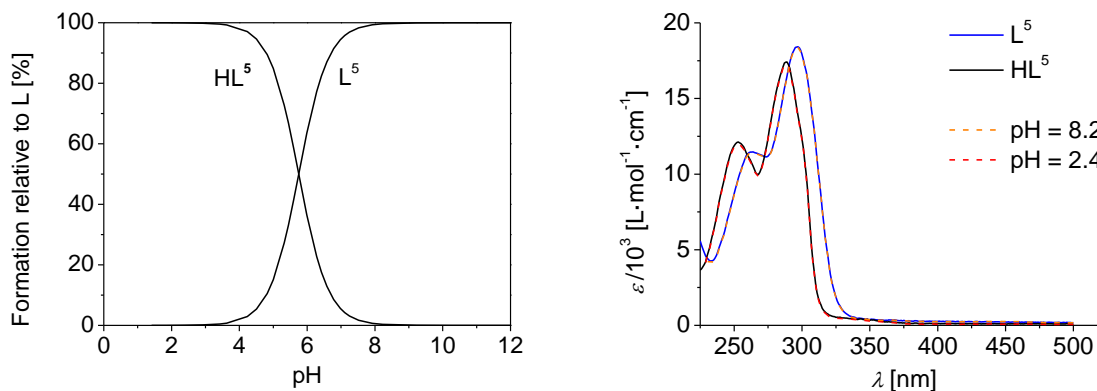


Figure S 27. Left: species distribution of the L^5 system in water; right: simulated and measured spectra of L^5 at different protonation states; $l = 0.1 \text{ M PO}_4^{3-}$, $[L^5] = 60 \mu\text{M}$. Charges are omitted for clarity.

5 was dissolved in 0.1 M phosphoric acid solution (water) and the solution's pH was adjusted to pH ~ 1.5 with KOH solution. Aliquots of KOH solution were added. The data were fitted by using *Spectfit*TM.^[11] The model and input parameters are shown in Table S 15.

The fit suggested that the complex is stable at pH = 2.5 and this would be in line with literature reports for the similar copper(II) complex $[\text{Cu}(\text{bim})_n]$ ($\text{bim} = 2,2'$ -bisimidazol, cf. $[\text{Cu}(\text{bim})_1]$: $\log\beta = 6.22$, $[\text{Cu}(\text{bim})_2]$: $\log\beta = 10.96$, above pH of 6 deprotonation and precipitation)^[13a] and to our observation that upon metal/ligand titration at pH = 2.5 small, reproducible changes occur. The complex stability constant is very similar to the one of $[\text{CuL}^1]$. However, there might be some doubts on the results, because (i) the standard deviation is high, (ii) $\text{p}K_{a,1}$ of 4.7 is lower than the one obtained for the closely related complex $[\text{Cu}(\text{impy})_3]$ ($\text{impy} = 2,2'$ -imidazolepyridine, cf. $\text{p}K_{a,1} = 7.9$, $\text{p}K_{a,2} = 9.0$, $\text{p}K_{a,2} = 11.3$)^[13], and (iii) the complex stability constant of $[\text{Cu}_2L^5]$ is higher than the one of $[\text{Cu}(\text{bim})_2]$ ^[13a]. We cannot perform potentiometric studies for further investigation of the stability constants, because the solubility of the ligand is too low in water.

Table S 15. Model and input parameters for the CuL^5 -system values marked with an asterisk have been obtained by fitting. Charges are omitted for clarity.

species $[\text{M}_x(\text{L})_y\text{H}_z]$	coloured	spectra fixed	value fixed	parameter	error
1 0 0 = Cu^{2+}	False		True	0	0
0 1 0 = L^5	True	True	True	0.0	0
0 1 1 = HL^5	True	True	True	5.75	0
1 1 0 = $[\text{CuL}^5]$	True	True	False	9.34066*	1.68340*
1 2 0 = 5	True	False*	False	22.0852*	1.44624*
1 2 -1 = 5H₁	True	False*	False	17.3768*	1.44636*
1 2 -2 = 5H₂	True	False*	False	8.39961*	1.44632*

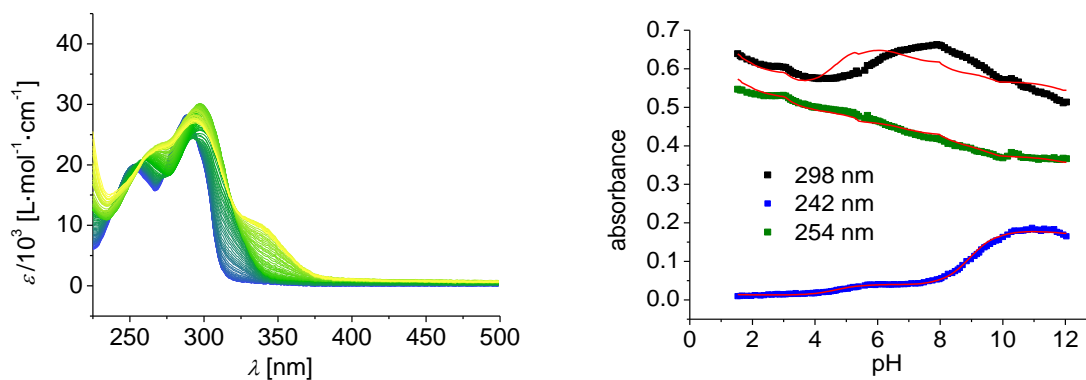


Figure S 28. Left: pH-dependent UV/Vis spectra of **5** in water; right: trend of the absorbance at three different wavelength (298 nm, 254 nm, and 254 nm), the red lines represent the fits; $I = 0.1 \text{ M PO}_4^{3-}$, $[\text{CuL}^5_2] = 30 \text{ }\mu\text{M}$.

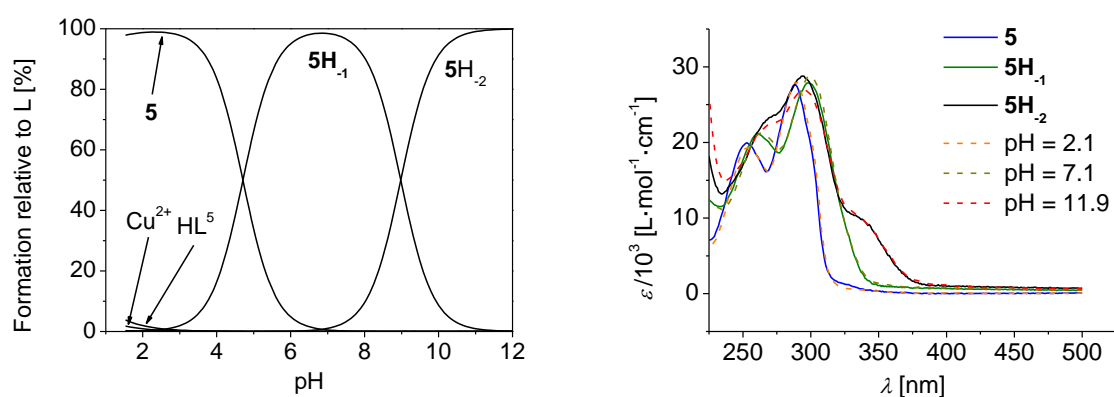


Figure S 29. Left: species distribution as calculated from the fit of the CuL^5 -system in water; right: simulated and measured spectra of the CuL^5 -system at different protonation states; $I = 0.1 \text{ M PO}_4^{3-}$, $[\text{CuL}^5_2] = 30 \text{ }\mu\text{M}$. Charges are omitted for clarity.

5) Electrochemical Studies

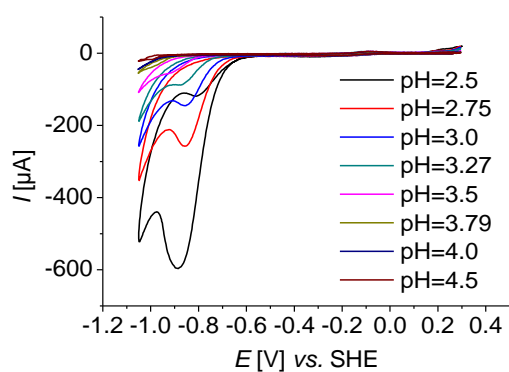


Figure S 30. pH-dependent CV measurements of **1a**, $[\mathbf{1a}] = 1 \text{ mM}$, $I = 0.1 \text{ M PO}_4^{3-}$, $\text{pH} = 2.5$, scan rate = 100 mVs^{-1} .

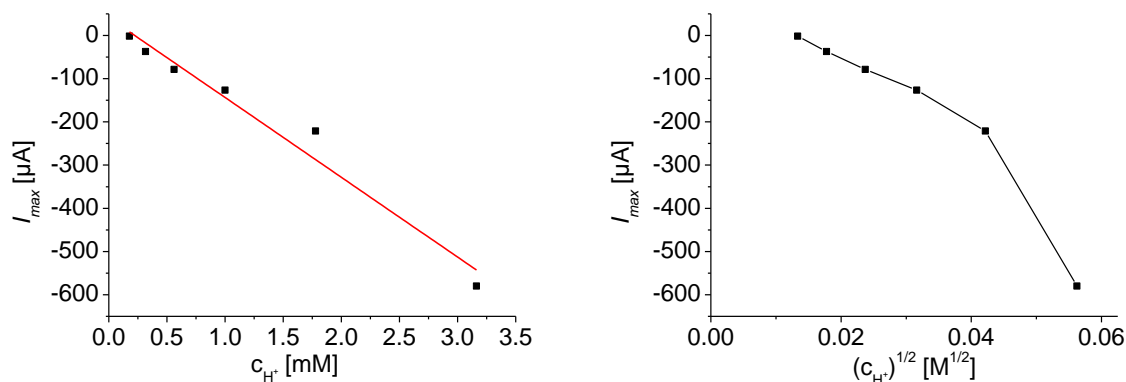


Figure S 31. Left: plot of the maximum current vs. proton concentration and the linear fit; right: plot of the maximum current vs. the square root of the proton concentration; conditions $[\mathbf{1a}] = 1 \text{ mM}$, $l = 0.1 \text{ M PO}_4^{3-}$, $\text{pH} = 2.5$, scan rate = 100 mVs^{-1} . A linear dependence of I_{max} on the proton concentration is indicative for second order kinetics, whereas a linear dependency of I_{max} on the square root of the proton concentration would imply first order kinetics.^[14]

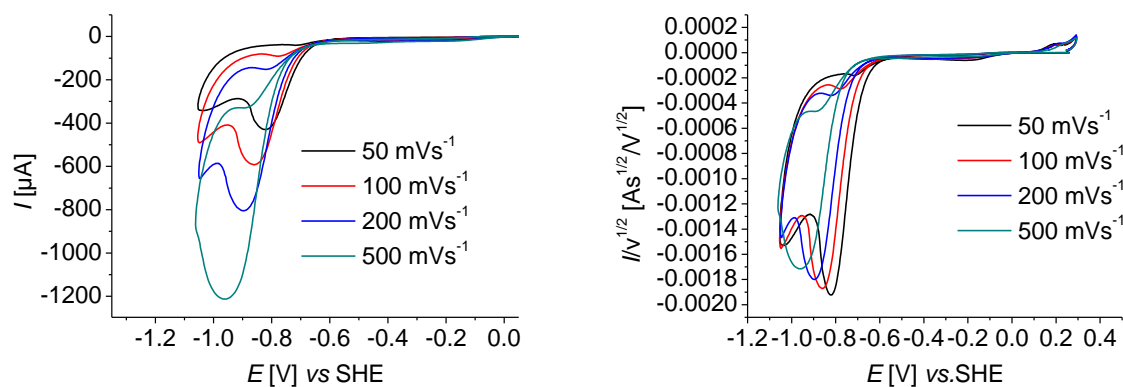


Figure S 32. Scan rate-dependent CV measurements of $\mathbf{1a}$, right: normalised plot ($I/v^{1/2}$); $[\mathbf{1a}] = 1 \text{ mM}$, $l = 0.1 \text{ M PO}_4^{3-}$, $\text{pH} = 2.5$.

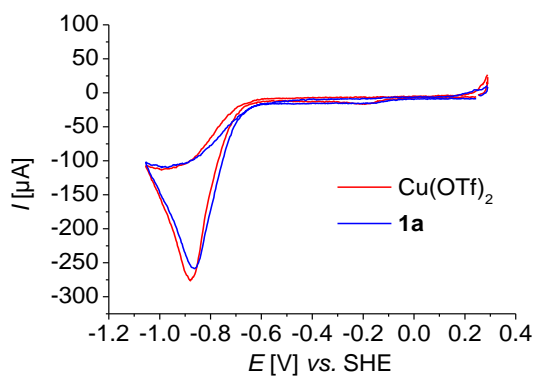


Figure S 33. CV measurements of $\mathbf{1a}$ and $\text{Cu}(\text{OTf})_2$ using sulphate buffer, $c = 1 \text{ mM}$, $l = 0.1 \text{ M SO}_4^{2-}$, $\text{pH} = 2.5$, scan rate = 100 mVs^{-1} .

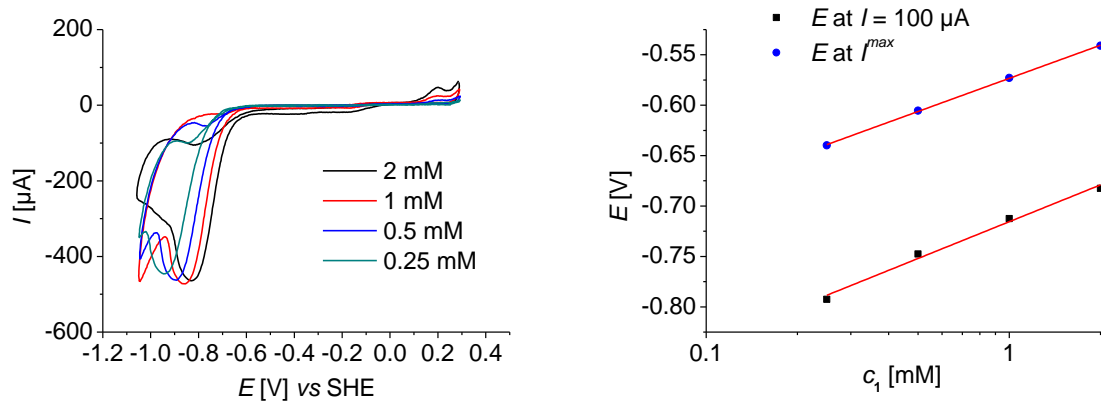


Figure S 34. Left: concentration-dependent CV measurements of **1a**, [**1a**] = see legend, $I = 0.1 \text{ M PO}_4^{3-}$, $\text{pH} = 2.5$, scan rate = 100 mVs^{-1} ; right: logarithmic plot of the potential at I^{max} and at $I = 100 \mu\text{A}$ vs. [**1a**].

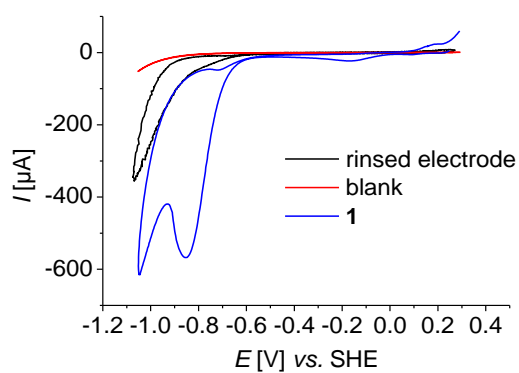


Figure S 35. Background of a copper free phosphate solution, representative cathodic scan, and scan of the electrode after 10 cathodic scans in a copper free phosphate solution; $I = 0.1 \text{ M PO}_4^{3-}$, $\text{pH} = 2.5$, scan rate = 100 mVs^{-1} , [**1a**] = 0.5 mM .

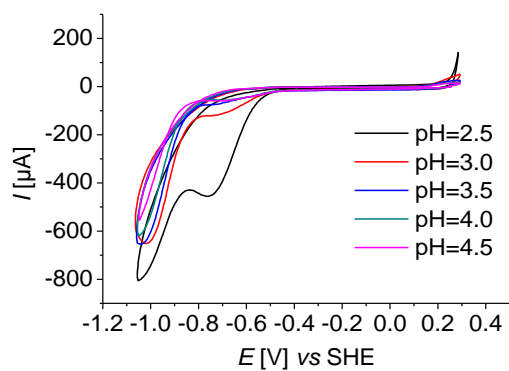


Figure S 36. pH-dependent CV measurements of a copper electrode; $I = 0.1 \text{ M PO}_4^{3-}$, $\text{pH} = 2.5$, scan rate = 100 mVs^{-1} .

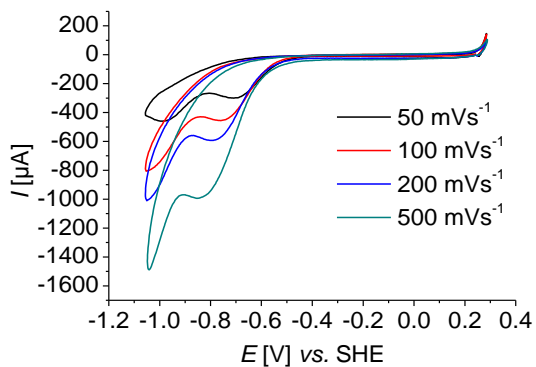


Figure S 37. Scan rate-dependent CV measurements of a copper electrode; $I = 0.1 \text{ M PO}_4^{3-}$, $\text{pH} = 2.5$.

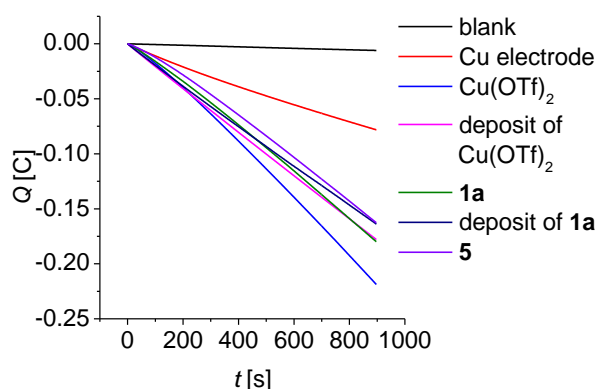


Figure S 38. CPE of **1a**, **5** and $\text{Cu}(\text{OTf})_2$ and CPE in a copper free solution of the deposits from a CPE of **1a** and $\text{Cu}(\text{OTf})_2$ $E^{\text{ap}} = -0.806 \text{ V}$. The plot shows the charge build-up versus time; $[c] = 0.5 \text{ mM}$, $I = 0.1 \text{ M PO}_4^{3-}$, $\text{pH} = 2.5$.

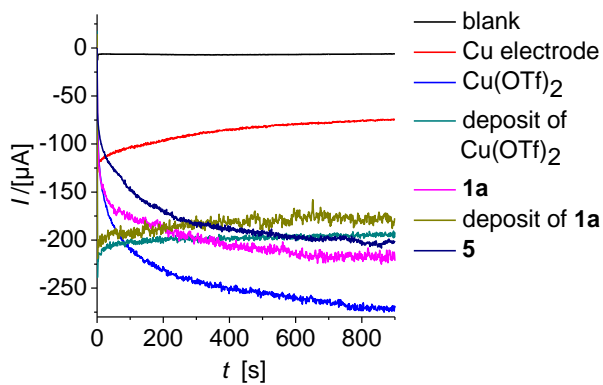


Figure S 39. Current vs. time plot for the CPE; $E^{\text{ap}} = -0.806 \text{ V}$, $[c] = 0.5 \text{ mM}$, $I = 0.1 \text{ M PO}_4^{3-}$, $\text{pH} = 2.5$.

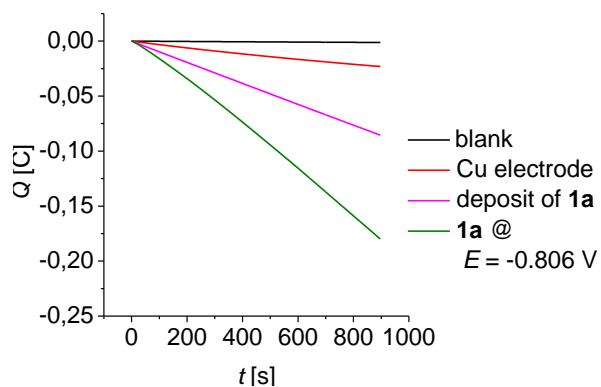


Figure S 40. CPE of a Cu electrode and the deposit after a CPE of **1a**, $E^{ap1} = -0.656$ V and initial deposition potential of **1a** $E = -0.806$ V. The plot shows the charge build-up versus time, $I = 0.1$ M PO_4^{3-} , $pH = 2.5$, $[1a] = 0.5$ mM.

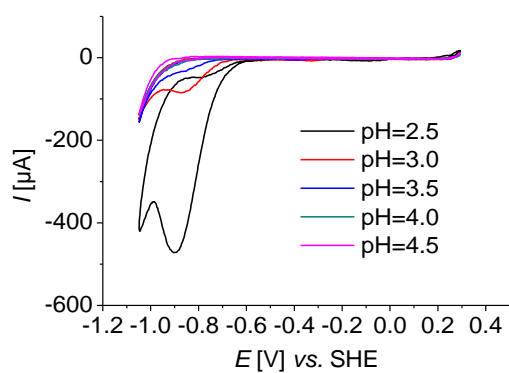


Figure S 41. pH-dependent CV measurements of **5**; $[5] = 0.5$ mM, $I = 0.1$ M PO_4^{3-} , $pH = 2.5$, scan rate = 100 mVs $^{-1}$.

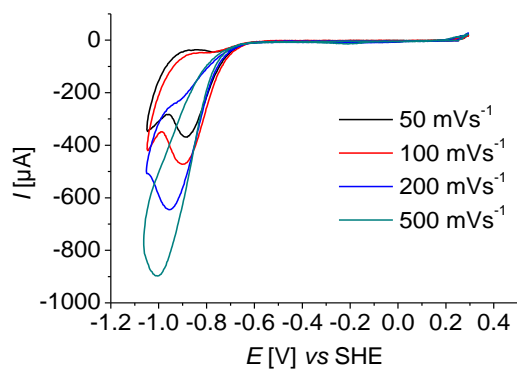


Figure S 42. Scan rate-dependent CV measurements of **5**; $[5] = 0.5$ mM, $I = 0.1$ M PO_4^{3-} , $pH = 2.5$.

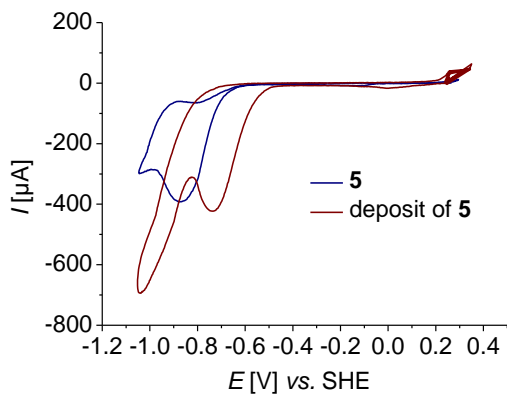


Figure S 43. CV data of 5 and the deposit of 5 after CPE at $E = -0.806$ V; $I = 0.1$ M PO_4^{3-} , $pH = 2.5$, scan rate = 100 mV s^{-1} .

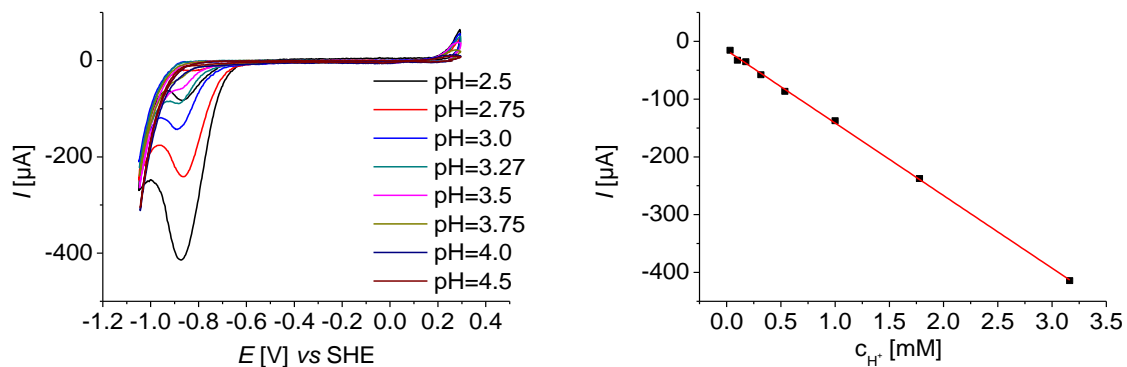


Figure S 44. Left: pH-dependent CV measurements of $Cu(OTf)_2$, $[Cu(OTf)_2] = 0.5$ mM, $I = 0.1$ M PO_4^{3-} , $pH = 2.5$, scan rate = 100 mV s^{-1} ; plot of the maximum current vs. proton concentration and the linear fit.

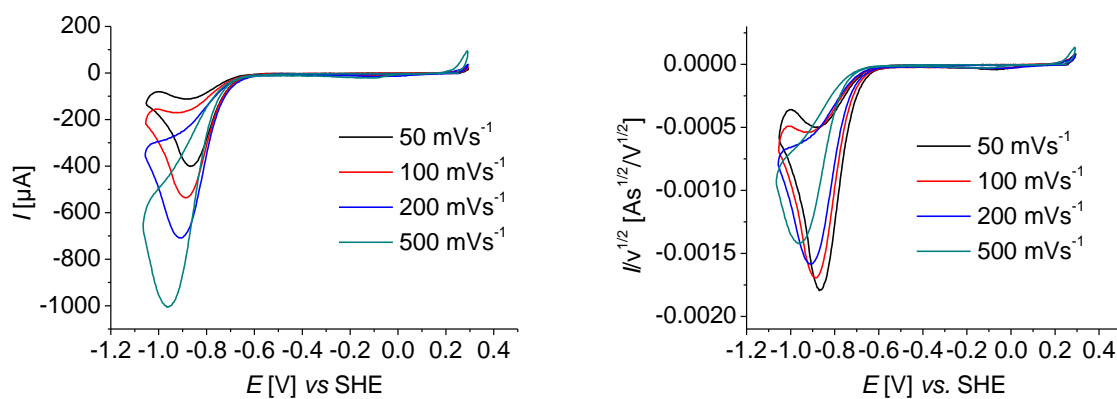


Figure S 45. Left: scan rate-dependent CV measurements of $Cu(OTf)_2$; right: normalised plot ($I/v^{1/2}$); $[Cu(OTf)_2] = 1.0$ mM, $I = 0.1$ M PO_4^{3-} , $pH = 2.5$.

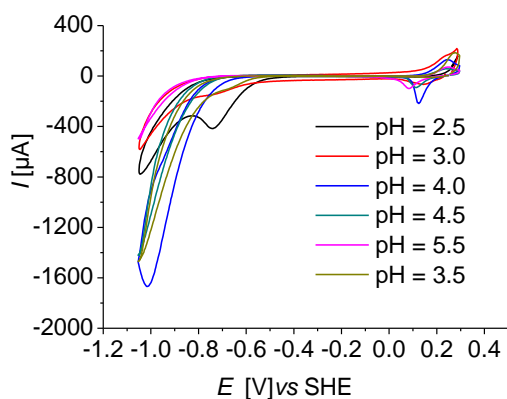


Figure S 46. pH-dependent CV measurements of the deposit of **1a**; $I = 0.1 \text{ M PO}_4^{3-}$, scan rate = 100 mVs^{-1} .

6) Electron Microprobe Analysis (EMPA)

a) Sample preparation

Sample Preparation of the CPE deposit: A GC plate (1 x 1 cm) was placed in a 1.0 mM solution of **1a** and $\text{Cu}(\text{OT})_2$, respectively, CPE was performed at $E = -0.806 \text{ V}$ for 15 min, the GC plate was washed carefully with Millipore water and dried at $60 \text{ }^\circ\text{C}$.

b) Measurement

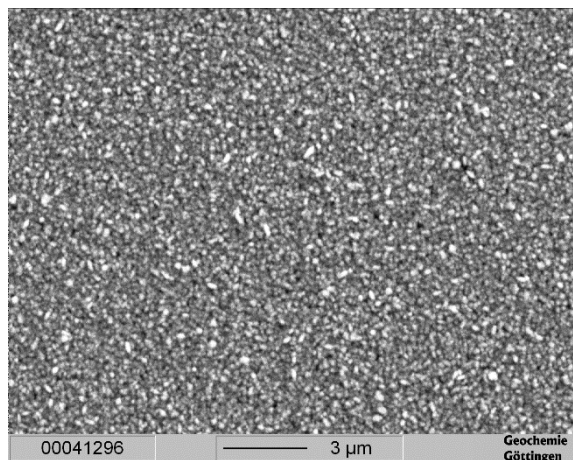


Figure S 47. Secondary electron image (SEI) of the electrode surface (carbon coated) showing the microcrystalline structure of the deposit after CPE of **1a**.

Measurements were carried out using a JEOL JXA8900 instrument equipped with 5 wavelength dispersive spectrometers (WDS). The beam conditions were set to an accelerating voltage of 15 kV, a beam current of 15 nA, and the beam diameter was varied between fully focused and $15 \text{ } \mu\text{m}$.

In order to calibrate the measurements, the mineral- and synthetic standards cuprite (Cu_2O), sanidine (KAlSi_3O_8), wollastonite (CaSiO_3), baryte (BaSO_4), apatite ($\text{Ca}_5\text{Cl}(\text{PO}_4)_3$), NaCl, topaz ($\text{Al}_2\text{F}_2\text{SiO}_4$) and Si_3N_4 were chosen to calibrate Cu, K, O, S, P, Cl, F and N respectively.

Quantification for Cu, K, O, S, P, Cl and F at different positions of the $\text{Cu}(\text{OTf})_2$ sample revealed an average atom ratio for Cu : O of $100 (\pm 5.4) : 14.7 (\pm 5.3)$ and none of the other elements were detected. Details of the measurements can be found in Table S 16.

Quantification for Cu, K, O, S, P, Cl, F and N at different positions of the sample of **1a** revealed an average atom ratio for Cu : O : N : Cl of 100 (± 1.8) : 6 (± 1.5) : 1.9 (± 0.3) : 7 (± 0.75) and none of the other elements were detected. Details of the measurements can be found in Table S 17. The chloride impurity may arise from leaking SCE because the buffer did not contain Cl atoms as checked by elemental analysis.

Tables of the measurements

Table S 16. $\text{Cu}(\text{OTf})_2$.

mass-%, normalised					atom-%				
Cu	O	P	Cl	K	Cu	O	P	Cl	K
96.6	2.99	0.21	0.05	0.12	88.5	10.86	0.39	0.08	0.18
96.3	3.38	0.19	<0.01	0.09	87.3	12.13	0.36	bdl	0.13
96.4	3.44	0.06	<0.01	0.07	87.4	12.37	0.10	bdl	0.10
93.9	5.48	0.35	<0.01	0.27	80.2	18.65	0.61	bdl	0.38
95.8	4.14	0.09	<0.01	<0.01	85.1	14.59	0.16	bdl	bdl
94.8	5.25	<0.01	<0.01	<0.01	81.8	18.00	bdl	bdl	bdl
93.7	6.33	<0.01	<0.01	<0.01	78.7	21.11	bdl	bdl	bdl
95.3	4.50	0.24	<0.01	<0.01	83.6	15.69	0.43	bdl	bdl
98.2	1.72	0.04	0.04	<0.02	93.3	6.51	0.09	0.06	bdl
97.7	2.25	0.03	0.05	0.03	91.4	8.37	0.05	0.08	0.04
96.4	3.09	0.23	0.08	0.16	88.0	11.19	0.43	0.12	0.24
97.3	2.40	0.12	0.05	0.10	90.6	8.87	0.23	0.09	0.16
97.9	1.97	0.05	0.04	<0.02	92.4	7.38	0.11	0.07	bdl

S always <0.02 %

Table S 17. **1a**.

mass-%, normalised					atom-%				
Cu	O	N	P	Cl	Cu	O	N	P	Cl
95.0	0.91	0.34	<0.01	3.71	88.9	3.37	1.44	bdl	6.23
94.7	0.94	0.33	<0.02	3.98	88.3	3.49	1.40	bdl	6.66
94.7	1.16	0.36	<0.02	3.71	88.0	4.27	1.52	bdl	6.17
94.8	1.20	0.39	<0.02	3.58	87.9	4.42	1.64	bdl	5.94
94.2	1.73	0.40	<0.01	3.58	86.1	6.26	1.67	bdl	5.86
94.9	1.22	0.34	<0.01	3.54	88.1	4.49	1.44	bdl	5.89
94.9	1.25	0.40	<0.01	3.38	88.0	4.61	1.69	bdl	5.60
94.6	1.30	0.36	<0.01	3.62	87.6	4.79	1.49	bdl	6.03
93.5	2.97	0.58	0.05	2.82	82.6	10.45	2.33	0.09	4.44
94.8	1.22	0.41	<0.01	3.54	87.9	4.50	1.72	bdl	5.86
94.9	1.27	0.38	<0.01	3.39	88.1	4.67	1.58	bdl	5.62
94.4	1.49	0.43	<0.02	3.67	86.7	5.44	1.78	bdl	6.07
94.7	1.32	0.39	<0.01	3.59	87.5	4.85	1.62	bdl	5.94
94.5	1.37	0.45	<0.01	3.58	87.0	5.01	1.90	bdl	5.93
94.3	1.46	<0.13	<0.01	3.88	87.0	5.34	bdl	bdl	6.41
95.2	1.34	<0.13	<0.01	3.19	88.5	4.94	bdl	bdl	5.33

95.6	1.09	0.38	<0.02	2.91	89.5	4.03	1.62	bdl	4.86
95.2	1.23	<0.12	<0.01	3.29	88.6	4.56	bdl	bdl	5.51
94.6	1.42	0.44	<0.01	3.52	87.1	5.20	1.83	bdl	5.80
94.9	1.31	0.39	<0.01	3.35	87.9	4.83	1.62	bdl	5.56
94.4	1.49	0.39	0.04	3.66	86.8	5.44	1.64	0.07	6.01
94.6	1.48	0.36	<0.01	3.57	87.1	5.41	1.52	bdl	5.91
94.9	1.43	<0.12	<0.01	3.29	87.9	5.27	bdl	bdl	5.45
94.6	1.53	<0.13	0.03	3.46	87.3	5.62	bdl	0.06	5.73
94.6	1.28	0.54	<0.01	3.57	87.1	4.69	2.27	bdl	5.91
93.9	1.58	0.48	<0.01	3.98	85.7	5.72	1.99	bdl	6.50
93.9	1.77	0.37	<0.01	3.94	85.6	6.41	1.52	bdl	6.45
93.6	1.87	0.43	<0.01	4.10	84.8	6.71	1.76	bdl	6.66
93.3	1.77	0.46	<0.01	4.44	84.5	6.38	1.88	bdl	7.22
92.6	2.12	<0.13	<0.01	4.86	83.2	7.54	bdl	bdl	7.83
93.5	1.56	0.47	0.04	4.42	85.1	5.64	1.93	0.07	7.21
94.1	1.32	0.42	<0.01	4.12	86.6	4.82	1.77	bdl	6.80
94.6	1.08	0.38	<0.02	3.93	87.9	3.98	1.62	bdl	6.54
95.2	0.95	0.31	<0.01	3.51	89.2	3.52	1.33	bdl	5.89

S<0.02 %, F<0.06 %

7) XPS Measurements

a) Sample Preparation

Dropcast sample: **1a** was dissolved in water, the solution was placed on the GC electrode (1x1 cm) and the water was evaporated at 60 °C.

CPE deposit: as described for EMPA.

b) Measurement

The X-ray photoemission spectroscopy (XPS) was measured using an Omicron EA 125 analyser and Mg K α (1253.6 eV) X-ray source. The data analysis was done using casaXPS software. All XPS spectra were calibrated using the graphitic carbon 1s peak of the underlying glassy carbon electrode (284.6 eV).^[15]

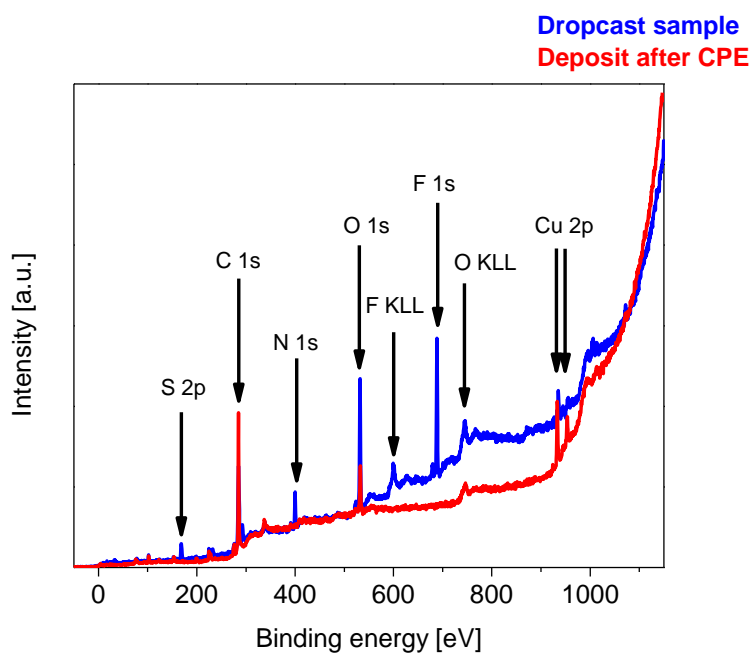


Figure S 48. Survey XPS spectra of a dropcast sample of **1a** on a glassy carbon electrode and of the glassy carbon electrode after CPE at an applied potential of -0.806 V.

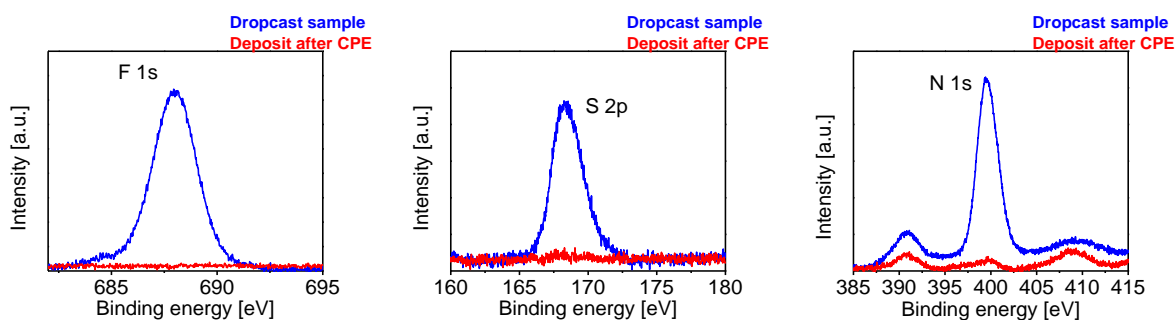


Figure S 49. High resolution XPS spectra of a dropcast sample of **1a** on a glassy carbon electrode and of the glassy carbon electrode after CPE at an applied potential of -0.806 V; peaks of F and S from the triflate anion are not present and only traces of nitrogen are left after CPE.

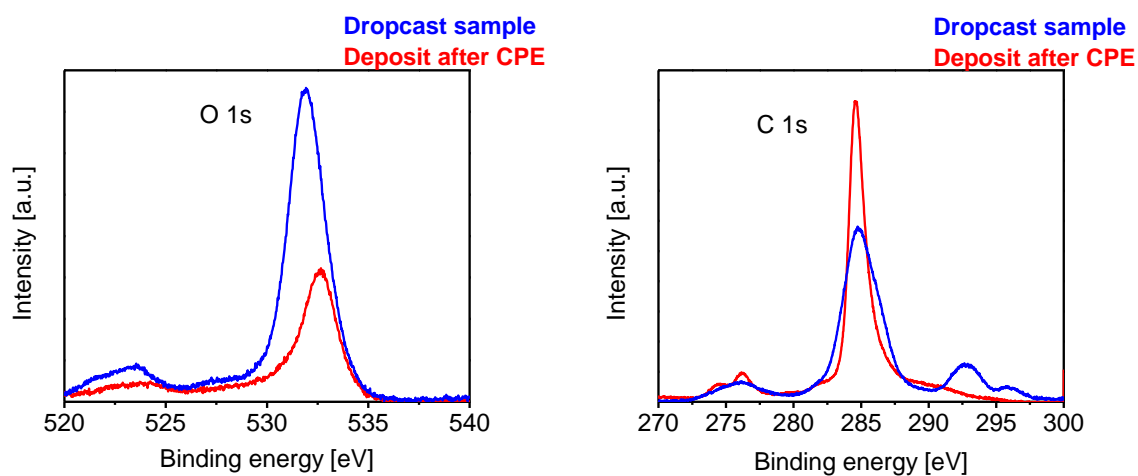


Figure S 50. High resolution XPS spectra of a dropcast sample of **1a** on a glassy carbon electrode and of the glassy carbon electrode after CPE at an applied potential of -0.806 V; the O 1s peak of the deposit is shifted compared to the respective peak of **1a**, which corroborates the Cu_2O formation and oxidation state.

8) References

- [1] M. Kügler, J. Gałęzowska, F. Schendzielorz, S. Dechert, S. Demeshko and I. Siewert, *Eur. J. Inorg. Chem.*, 2015, 2695.
- [2] C. H. Rochester, *J. Chem. Soc., Dalton Trans.*, 1972, 5.
- [3] a) B. Chiswell, F. Lions and B. S. Morris, *Inorg. Chem.*, 1964, **3**, 110; b) Z. Liu, T. Ouyang, H. Cho; Y. Goti, B. Feldman, F. Mao and A. Heller, U.S. Pat. Appl. Publ., 20090099434.
- [4] U. S. Schubert, E. Eschbaumer and M. Heller, *Org. Lett.*, 2000, **2**, 3373.
- [5] M. G. Miles, G. Doyle, R. P. Cooney and R. S. Tobias, *Spectrochim. Acta Part A Mol. Spectrosc.*, 1969, **25**, 1515.
- [6] G. M. Sheldrick, *Acta Crystallogr. Sect. A*, 2008, **64**, 112.
- [7] *X-Red*, STOE & Cie GmbH: Darmstadt, Germany, 2002.
- [8] P. Gans and A. Sabatini, A. Vacca, *Talanta*, 1996, **43**, 1739.
- [9] P. Gans, *Data Fitting in the Chemical Sciences: by the Method of Least Squares*; John Wiley & Sons: Chichester, U.K, 1992.
- [10] L. Alderighi, P. Gans, A. Ienco, D. Peters, A. Sabatini and A. Vacca, *Coord. Chem. Rev.*, 1999, **184**, 311.
- [11] R. A. Binstead, A. D. Zuberbühler and B. Jung, *Spectfit*, version 3.0.38; Windows; Spectrum Software Associates: Chapel Hill, NC, 2006.
- [12] a) I. Török, P. Surdy, A. Rockenbauer, L. Korecz Jr, G. J. Anthony A. Koolhaas and T. Gajda, *J. Inorg. Biochem.*, 1998, **71**, 7; b) H. Sigel, A. Saha, N. Saha, P. Carloni, L. E. Kapinos and R. Griesser, *J. Inorg. Biochem.*, 2000, **78**, 129; c) S. S. Babić, A. J. M. Horvat, D. Mutavdžić Pavlović and M. Kaštelan-Macan, *Anal. Chem.*, 2007, **26**, 1043.
- [13] R. K. Boggess and R. B. Martin, *Inorg. Chem.*, 1974, **13**, 1525.
- [14] The electrochemical current is proportional to the square root of the substrate concentration: $i_c = Fc_p\sqrt{D_p k c_A}$. F is the Faraday constant, c_p the concentration of the redox catalyst, D_p its diffusion coefficient, k the rate constant and c_A the concentration of the substrate. Thus, a linear dependence of the current on the substrate concentration can be regarded as a process with second-order kinetics. See for example: a) J. M. Savéant, K. Su, *J. Electroanal. Chem.*, 1984, **171**, 341; b) J. M. Savéant, *Chem. Rev.*, 2008, **108**, 2348.
- [15] A. Dekanskia, J. Stevanovic, R. Stevanovic, B. Nikolic and V. M. Jovanovic, *Carbon*, 2001, **39**, 11955.